

Status of Super charm-tau factory project

LOGASHENKO IVAN (BINP, NOVOSIBIRSK)

13TH INTERNATIONAL WORKSHOP ON E+E- COLLISIONS FROM PHI TO PSI

Partially supported by RSF grant 19-72-20114

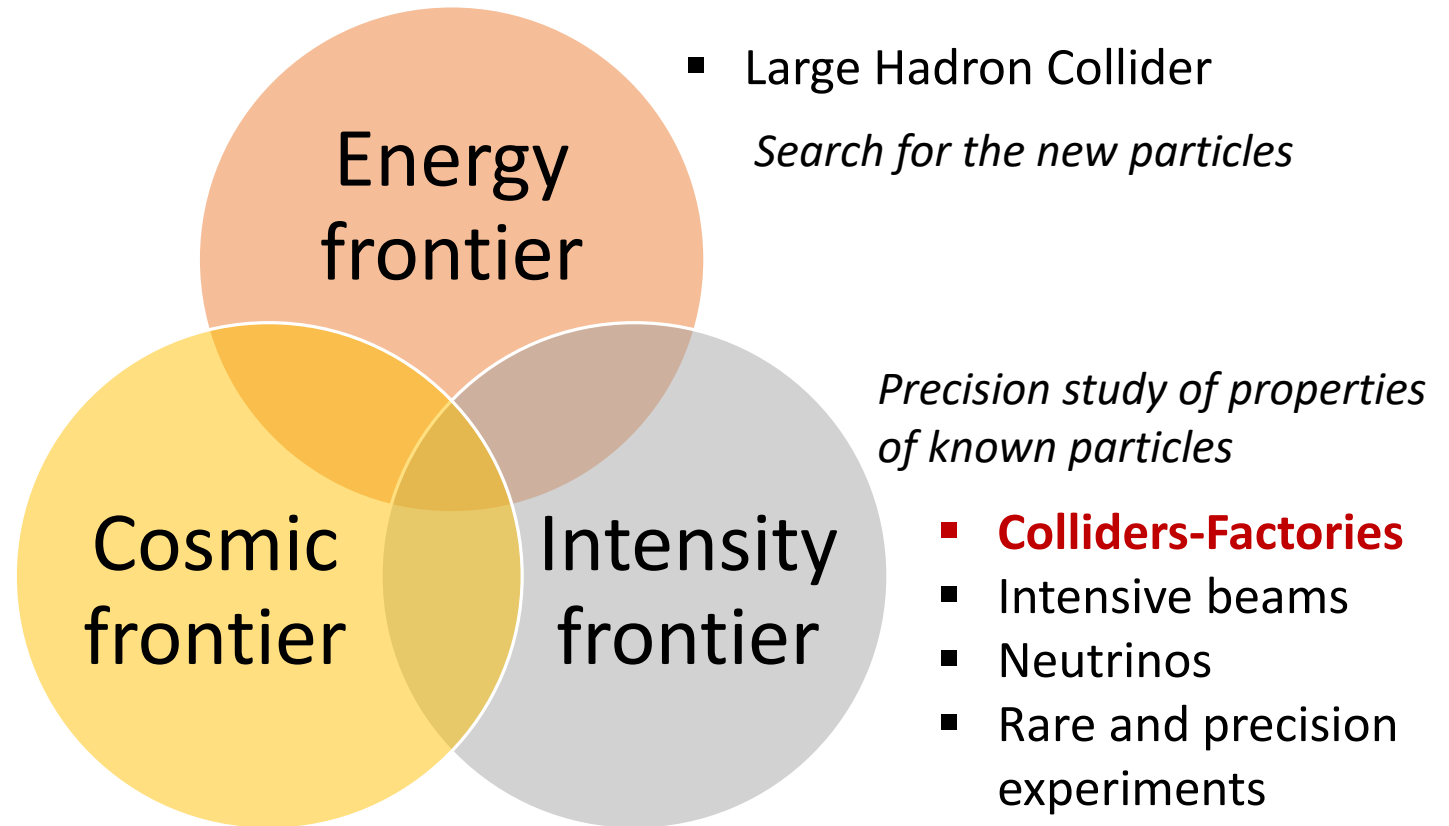
Motivation

The global strategy for the particle physics

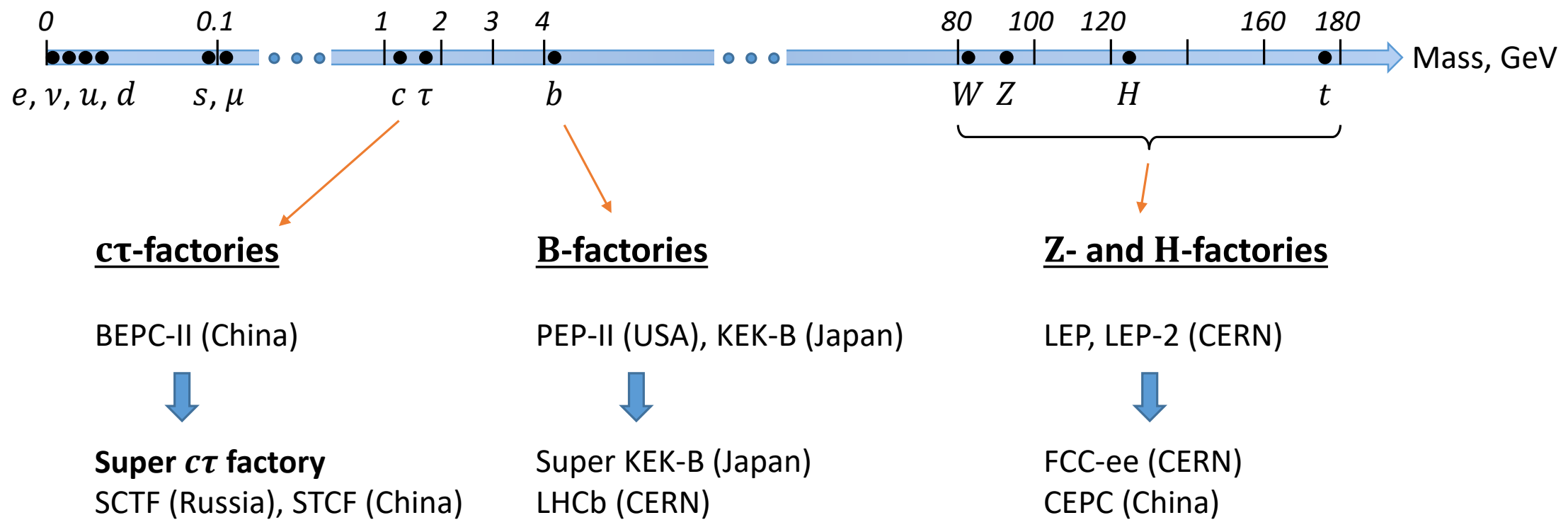
After the discovery of Higgs boson, the particle physics is focused on the deep understanding of the predictions of the Standard Model and on the search of phenomena beyond SM

There are many roads...

- Dark matter
- Cosmic rays
- Space-based experiments



Colliders-Factories



Energy ranges of high luminosity colliders (factories) correspond to production thresholds of known particles.
Ultimate performance (precision) is determined by luminosity and detector quality

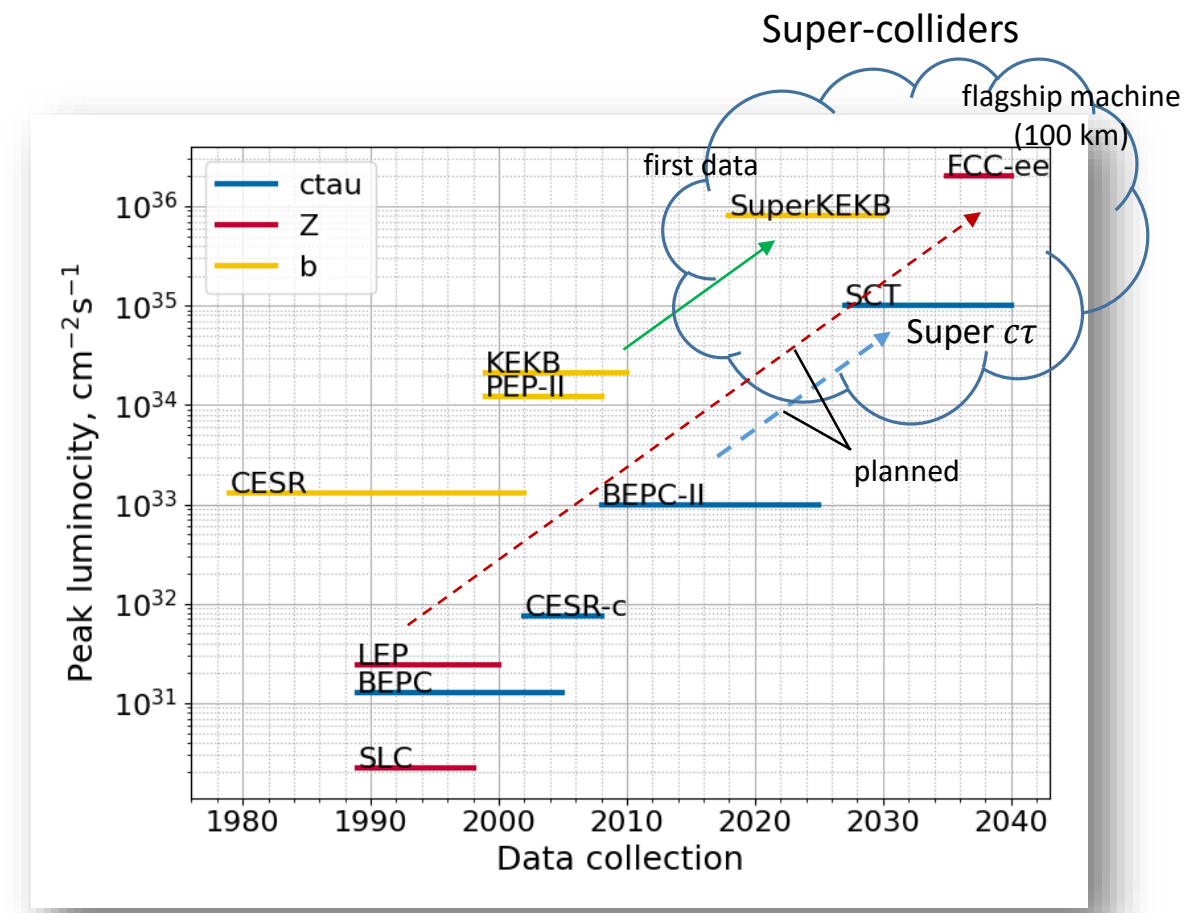
Generations of colliders-factories

Today:

	Tomorrow:
LHCb: 5 fb^{-1}	$\xrightarrow{x10-60}$ LHCb: $50/300 \text{ fb}^{-1}$ (Run 3/4)
B-factories: 1 ab^{-1}	$\xrightarrow{x50}$ Super KEK-B: 50 ab^{-1}
BES-III: $\sim 100 \text{ fb}^{-1}$	$\xrightarrow{x100}$ Super C-tau factory: $\sim 10 \text{ ab}^{-1}$

- There is balance/synergy between existing $c\tau$ -factory (BES-III) and B -factories (BABAR, BELLE, LHCb)
- New generation B -factories started data taking (BELLE-2, LHCb)
- To keep balance, there is place for the new generation $c\tau$ -factory

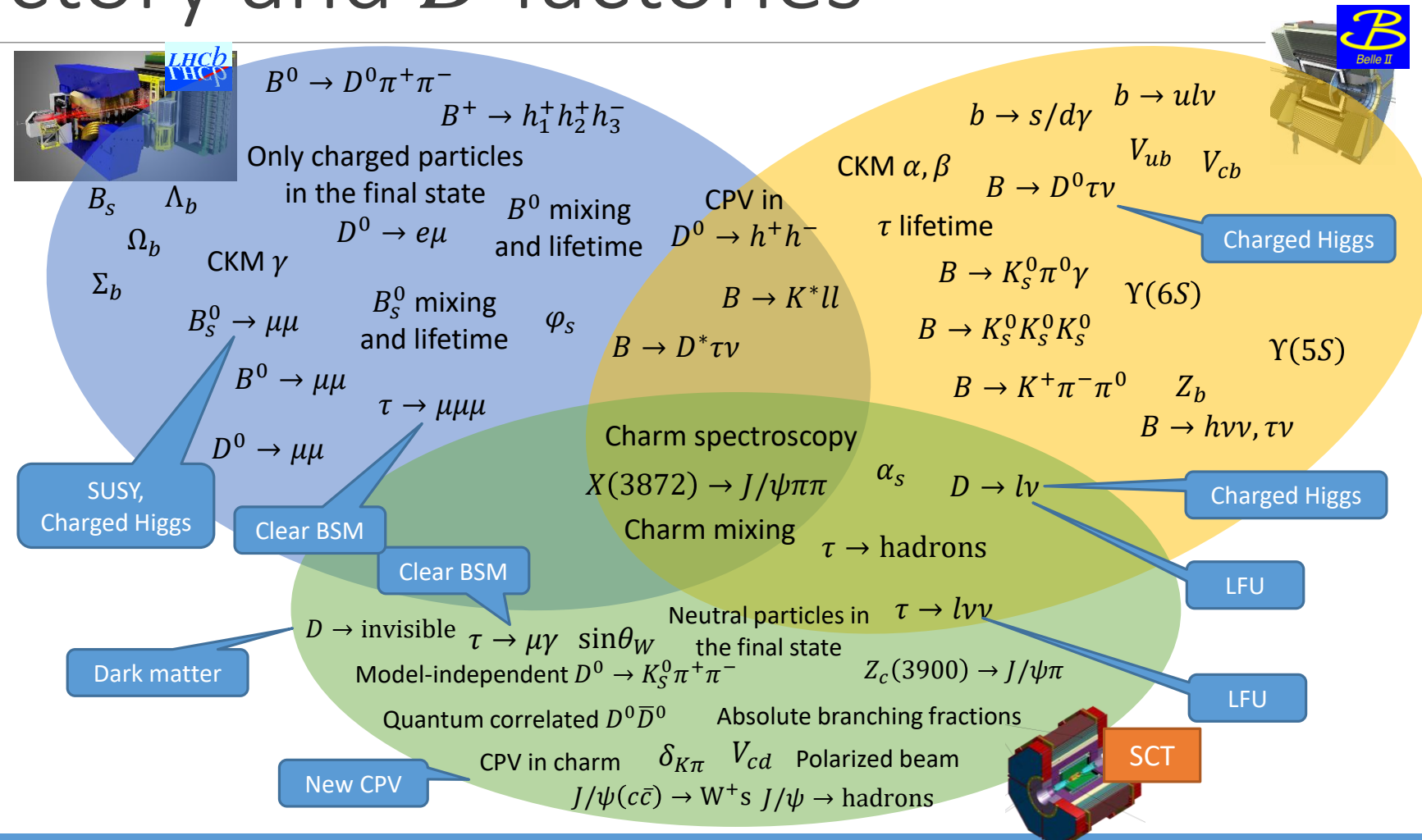
Super $c\tau$ -factory is the natural part of the global particle physics strategy



Super $c\tau$ factory and B factories

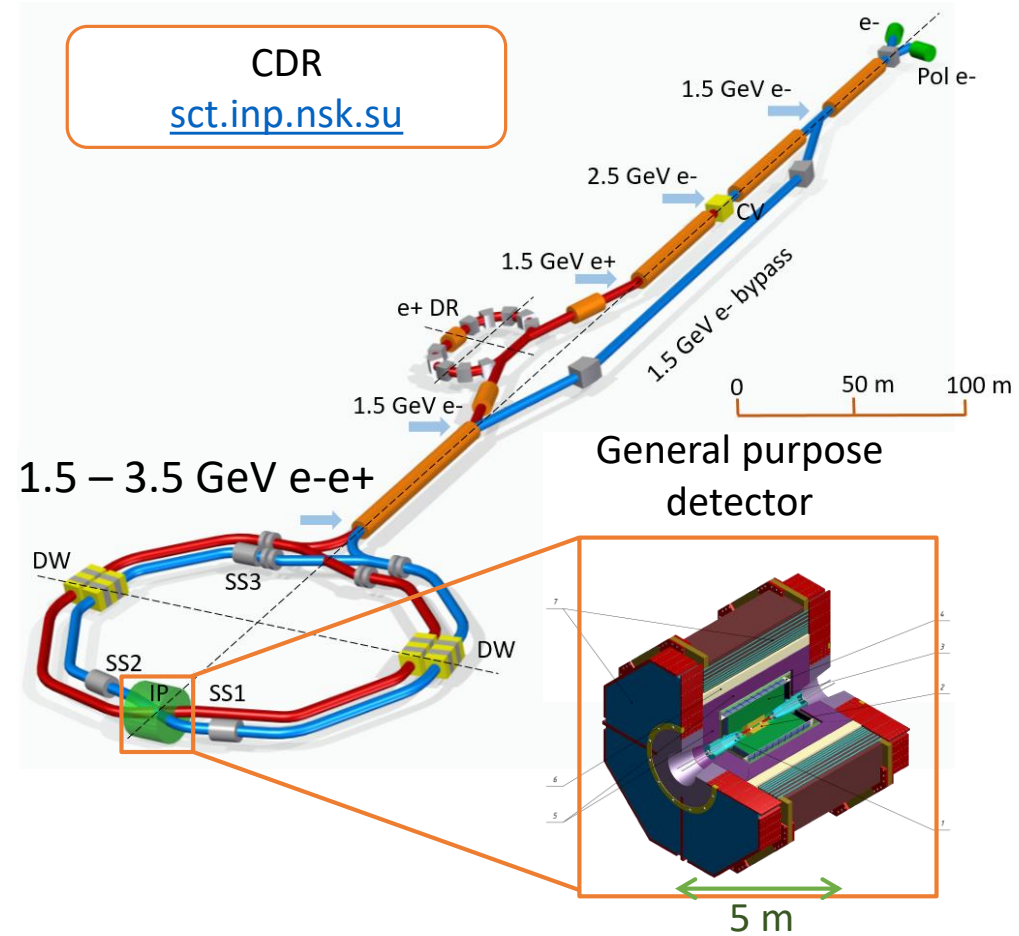
The experiments at Super charm-tau factory are complement to experiments at Super KEK-B and LHCb, with unique possibilities:

- Threshold production of particles
- Pair production
- Quantum correlations in $D^0\bar{D}^0$ production
- Low multiplicity, full reconstruction of decay chain
- Polarization of electron beam



Super charm-tau factory

- Super charm-tau factory is e^+e^- collider, dedicated to precision study of properties of charm-quark, tau-lepton, study of strong interactions, search of BSM physics
 - Beam energy from 1.5 (1.0) to 3.5 GeV
 - Luminosity $\mathcal{L} = 10^{35} \text{ cm}^{-2}\text{c}^{-1}$ @ 2 GeV
 - Longitudinally polarized electron beam
- Experiments will be conducted using state-of-the-art general purpose detector
 - Tracking (including low p_t)
 - Calorimetry (high resolution, fast, π^0/γ sep.)
 - Particle ID ($\mu/\pi/K/p$ up to 1.5 GeV/c)

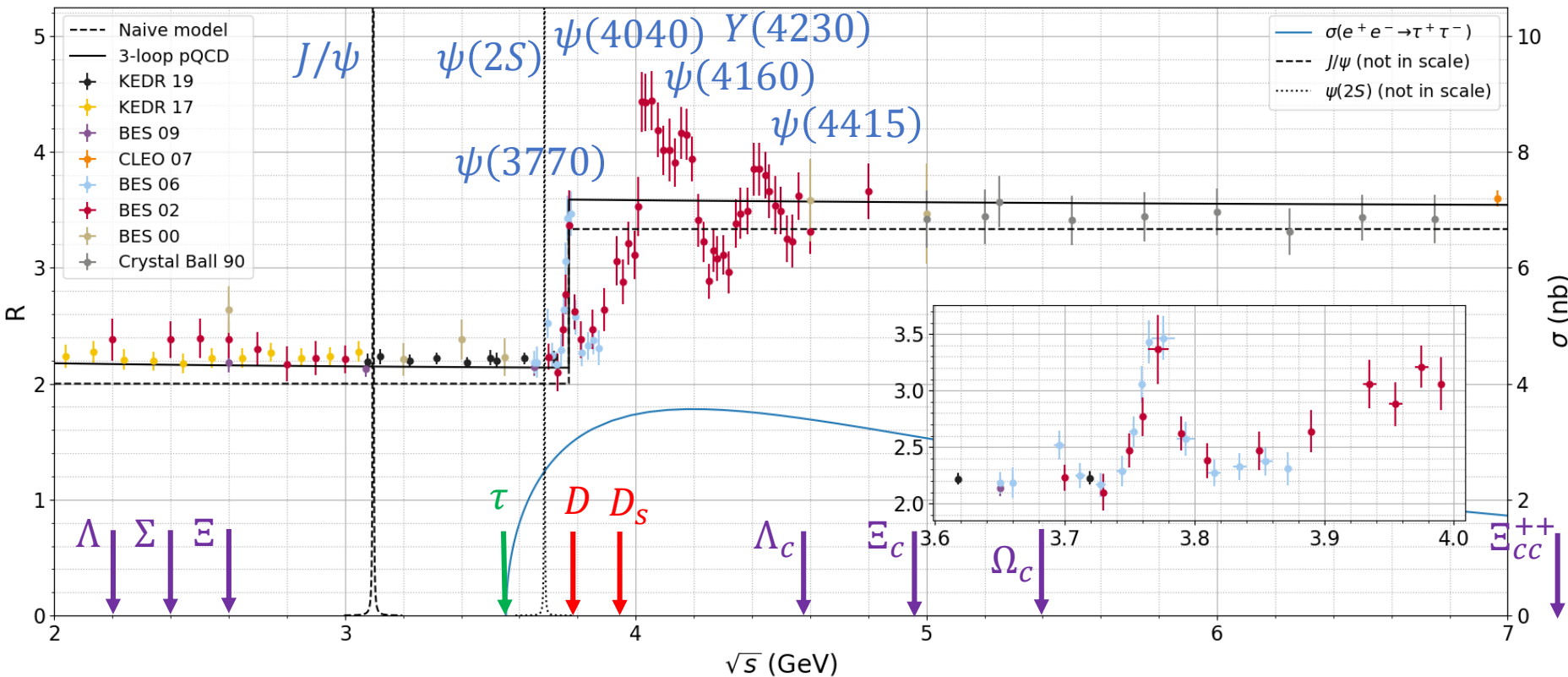


Physics program

SCTF energy range

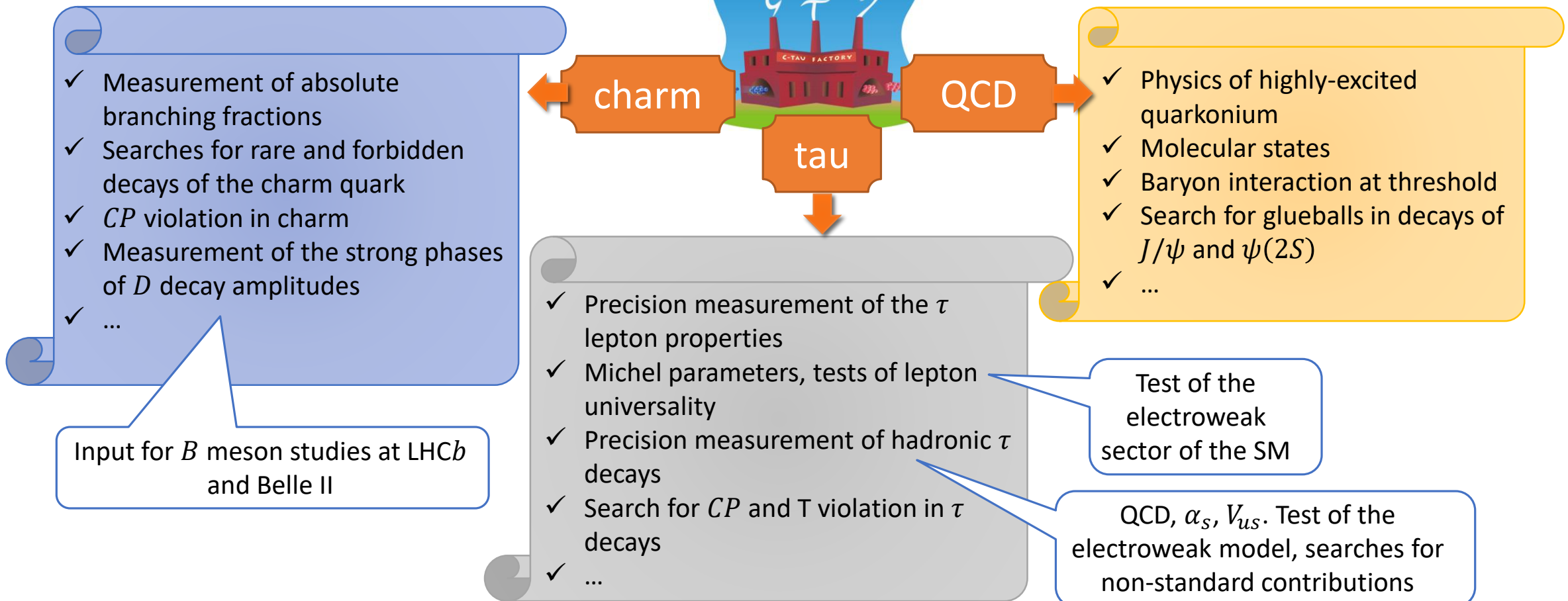
$$R \equiv \frac{\sigma(e^+e^- \rightarrow \text{hadrons})}{\sigma_0(e^+e^- \rightarrow \mu^+\mu^-)}$$

Threshold production of nonrelativistic particles provides best conditions for their comprehensive study

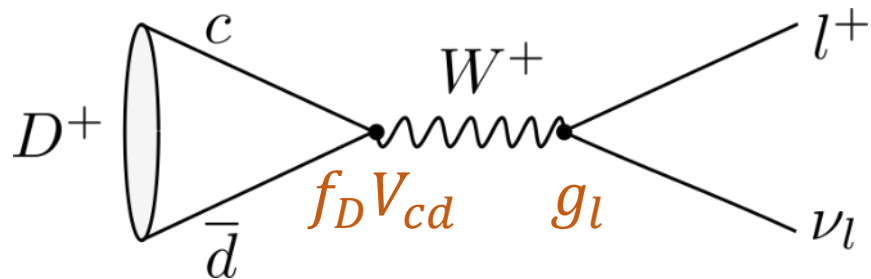


$\mathcal{L} = 10^{35} \text{ cm}^{-2} \text{s}^{-1}$
A one-year dataset

Overview of SCTF physics



(Semi-)leptonic $D_{(s)}$ decays

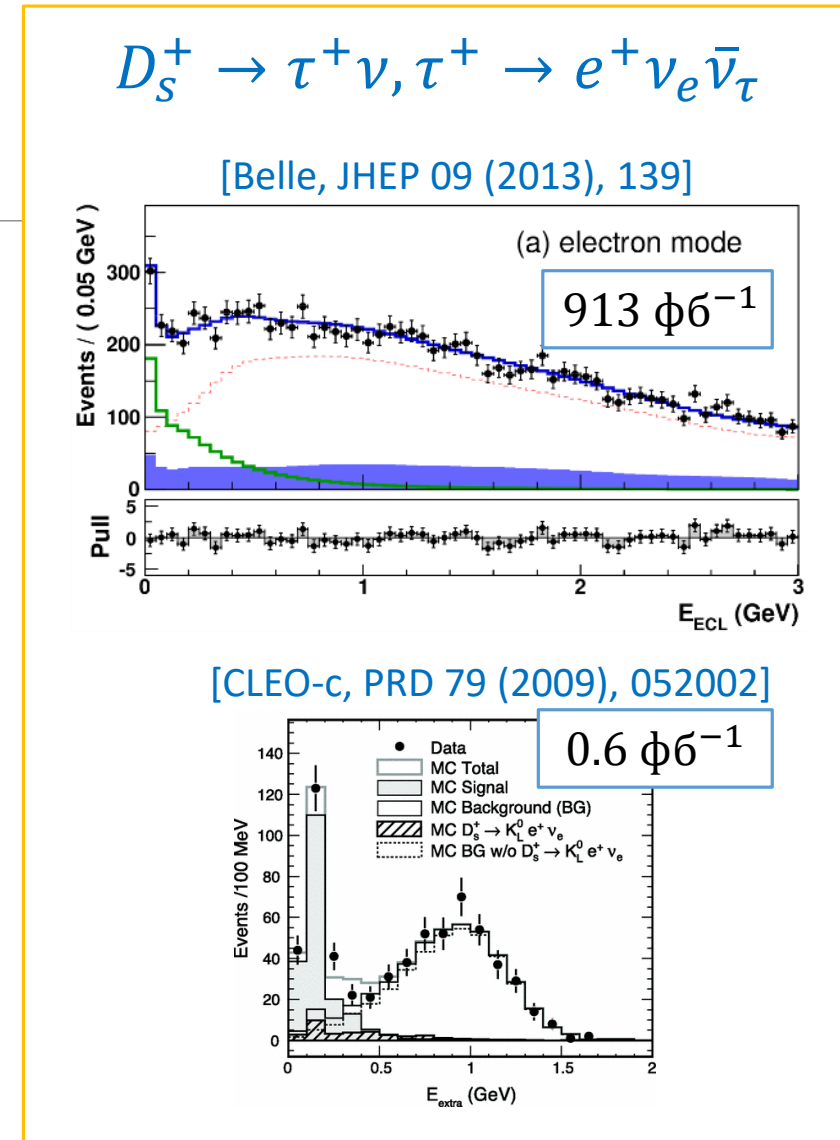


$$\Gamma(D^+ \rightarrow l\nu) = \frac{G_F^2}{8\pi} f_D^2 m_l^2 m_D \left(1 - \frac{m_l^2}{m_D^2}\right) |V_{cd}|^2$$

- Branchings measurement: f_D , V_{cd} , V_{cs}
- Lepton universality test

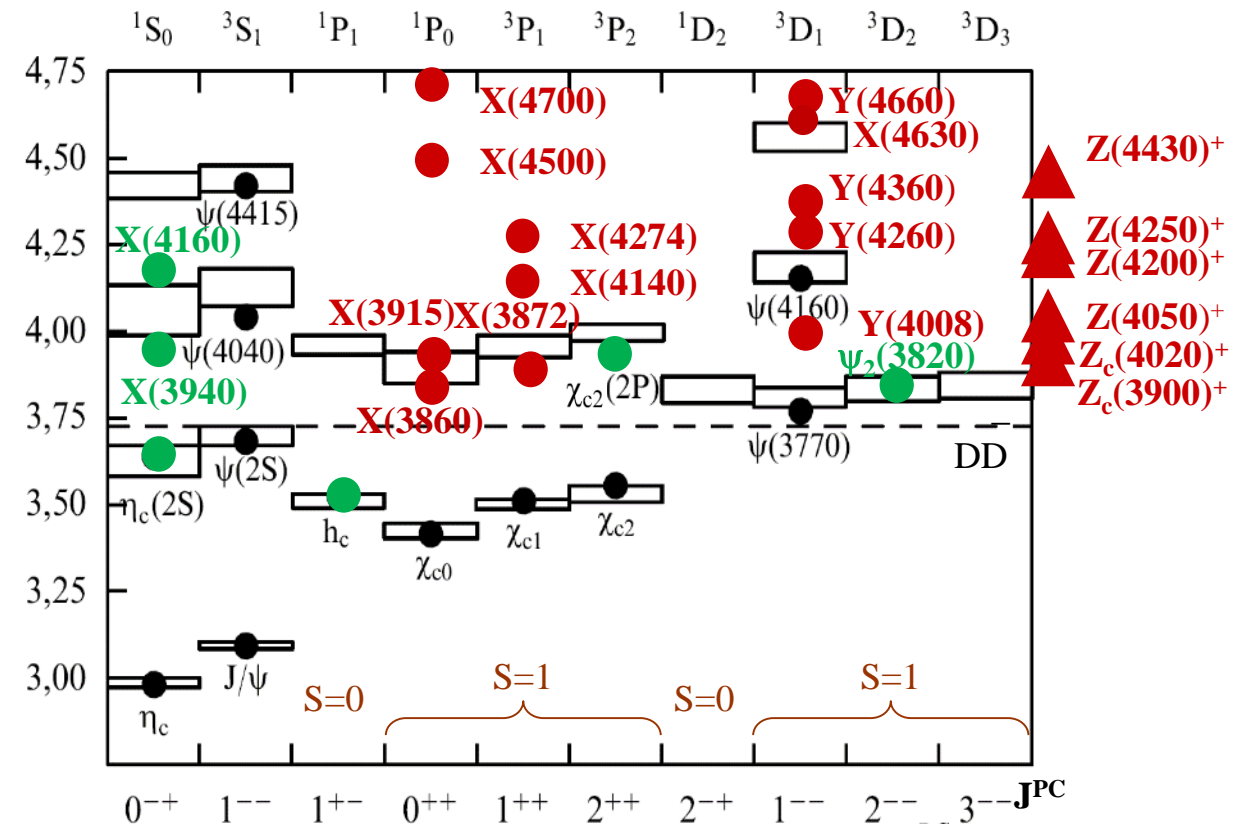
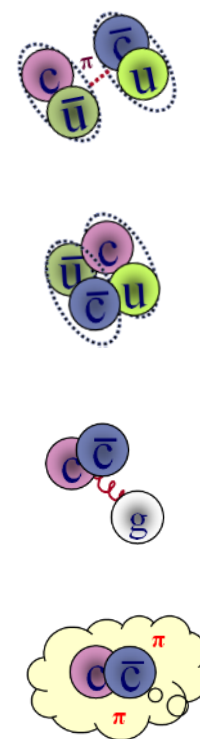
Table 1: LFU test at BESIII with (semi)leptonic D decays.

	$R(D_s^+)$	$R(D^+)$	$R(K^-)$	$R(\bar{K}^0)$	$R(\pi^-)$	$R(\pi^0)$
SM	9.74(1)	2.66(1)	0.975(1) [31]	0.975(1) [31]	0.985(2) [31]	0.985(2) [31]
BESIII	9.98(52)	3.21(64)	0.978(14)	0.988(33)	0.922(37)	0.964(45)



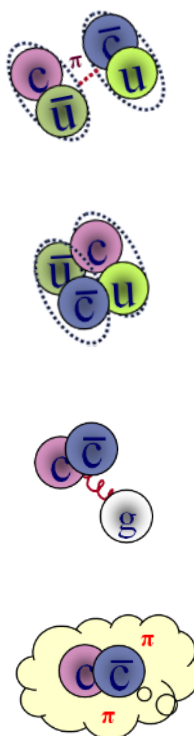
Detailed study of the charmonium-like states

- Existing QCD laboratory
- Cross sections to be measured:
 - $e^+e^- \rightarrow J/\psi\pi^+\pi^-$
 - $e^+e^- \rightarrow J/\psi\pi^0\pi^0$
 - $e^+e^- \rightarrow \psi(2S)\pi^+\pi^-$
 - $e^+e^- \rightarrow D\bar{D}, D^*\bar{D}, \dots$
 - $e^+e^- \rightarrow D\bar{D}\gamma$
 - $e^+e^- \rightarrow D\bar{D}(n\pi)$
 - $e^+e^- \rightarrow D_s^+D_s^-$
 - $e^+e^- \rightarrow D_s^+D_s^-(n\pi)$
 - $e^+e^- \rightarrow \Lambda_c\bar{\Lambda}_c$
 - ...

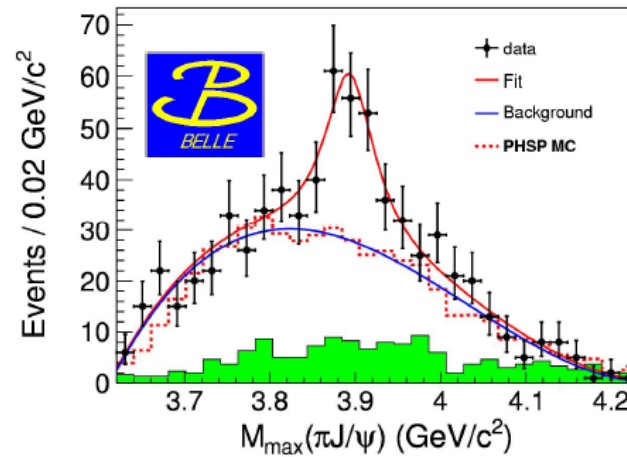


Detailed study of the charmonium-like states

- Existing QCD laboratory
- Cross sections to be measured:
 - $e^+e^- \rightarrow J/\psi\pi^+\pi^-$
 - $e^+e^- \rightarrow J/\psi\pi^0\pi^0$
 - $e^+e^- \rightarrow \psi(2S)\pi^+\pi^-$
 - $e^+e^- \rightarrow D\bar{D}, D^*\bar{D}, \dots$
 - $e^+e^- \rightarrow D\bar{D}\gamma$
 - $e^+e^- \rightarrow D\bar{D}(n\pi)$
 - $e^+e^- \rightarrow D_s^+D_s^-$
 - $e^+e^- \rightarrow D_s^+D_s^-(n\pi)$
 - $e^+e^- \rightarrow \Lambda_c\bar{\Lambda}_c$
 - ...

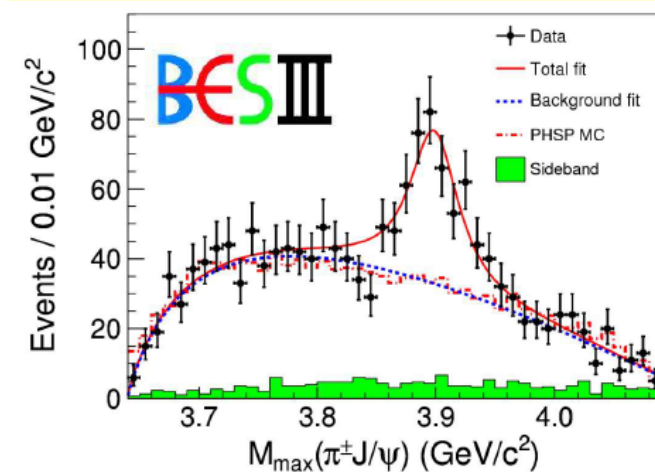


Belle with ISR: PRL110, 252002
967 fb⁻¹ in 10 years running time



- $M = 3894.5 \pm 6.6 \pm 4.5$ MeV
- $\Gamma = 63 \pm 24 \pm 26$ MeV
- 159 ± 49 events
- $>5.2\sigma$

BESIII at 4.260 GeV: PRL110, 252001
0.525 fb⁻¹ in one month running time

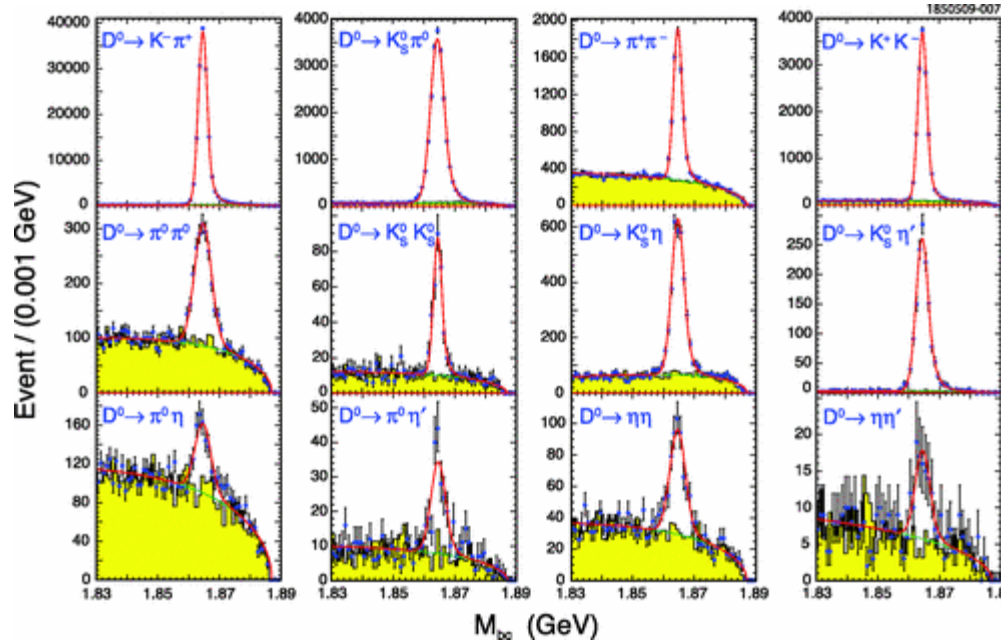


- $M = 3899.0 \pm 3.6 \pm 4.9$ MeV
- $\Gamma = 46 \pm 10 \pm 20$ MeV
- 307 ± 48 events
- $>8\sigma$

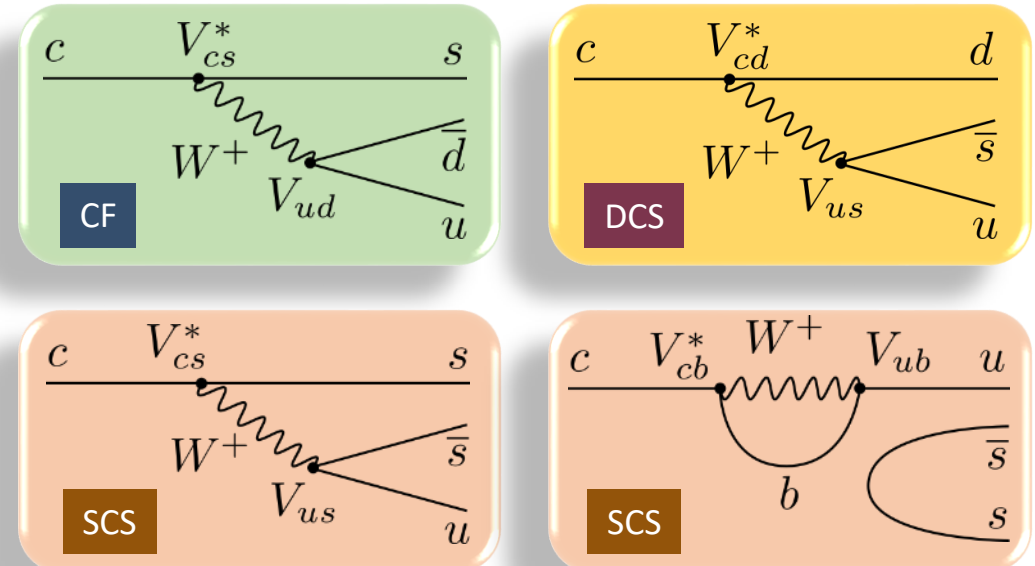
10 years vs. 0.1 year vs. 1 day at SCT

CPV in charm

- Measurement of CP asymmetries in decays of D^0 , D^+ , D_s^+ at the precision level of $\sim 10^{-4}$
 - Advantage of full event reconstruction
 - Coherent $D^0\bar{D}^0$ pairs



CLEOc 0.818 fb^{-1} @ 3774 MeV [PRD 81, 052013 (2010)]



$$\Delta A_{CP} = (-15.4 \pm 2.9) \times 10^{-4}$$

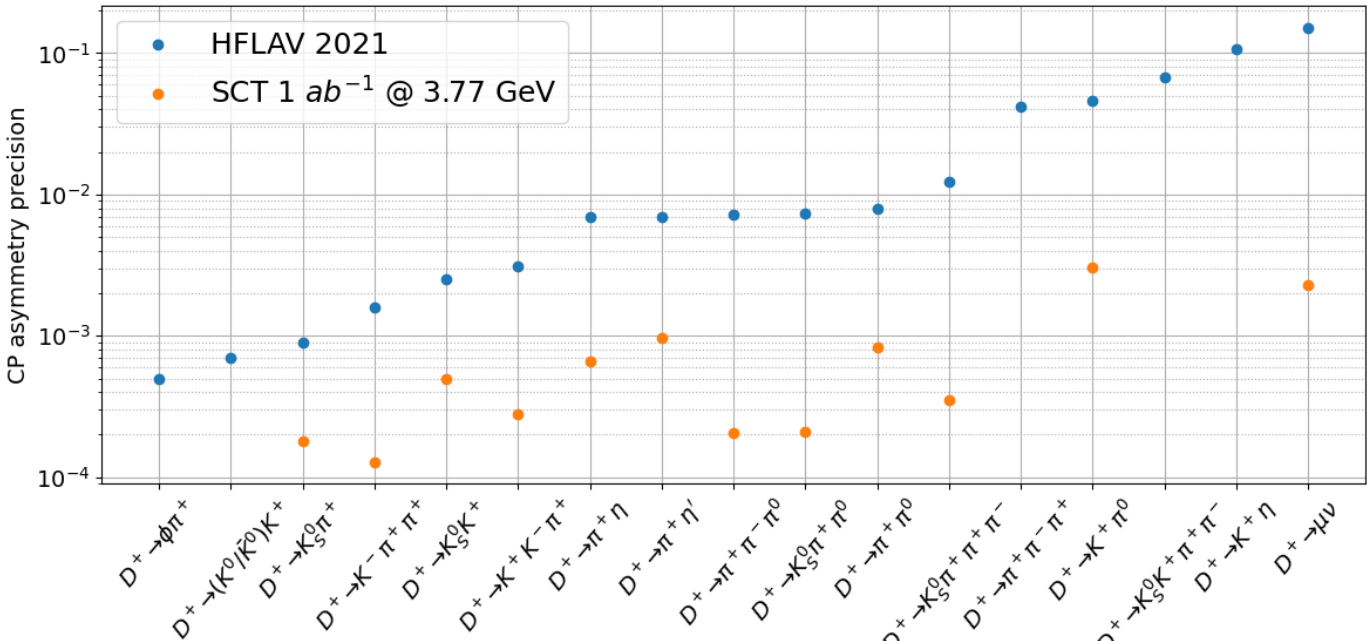
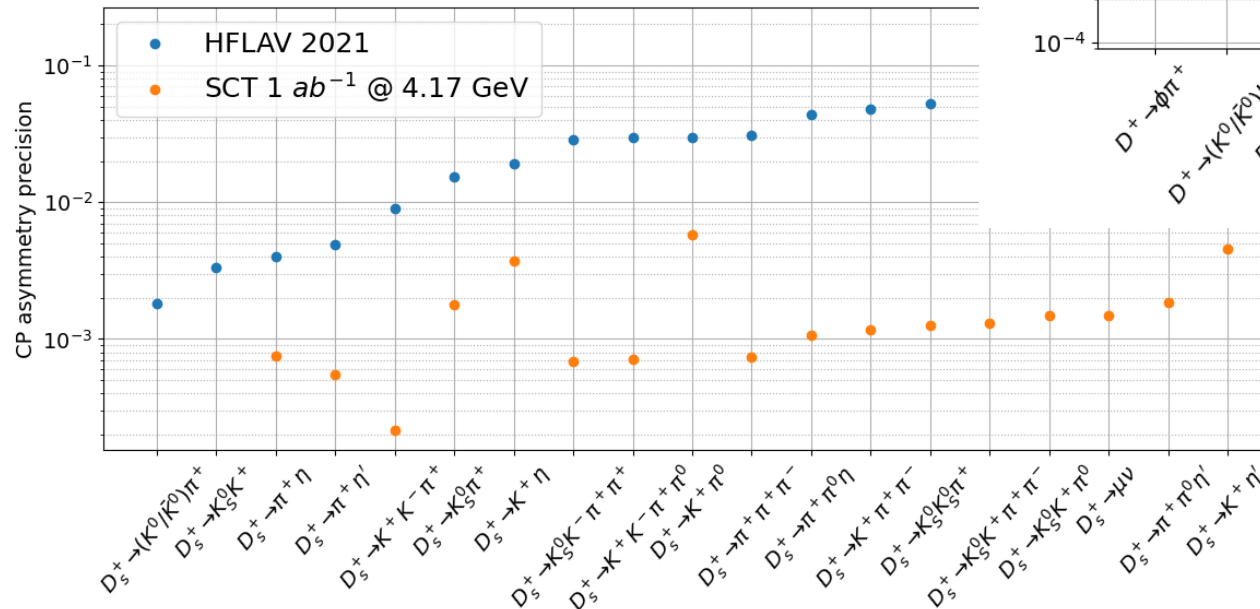
$$D^0 \rightarrow h^+ h^-$$



2019

CPV in charm

- The only experiment able to observe CP-asymmetry in D -mesons decays at the level of $\mathcal{O}(10^{-3})$ simultaneously in many final states, including states with neutrals



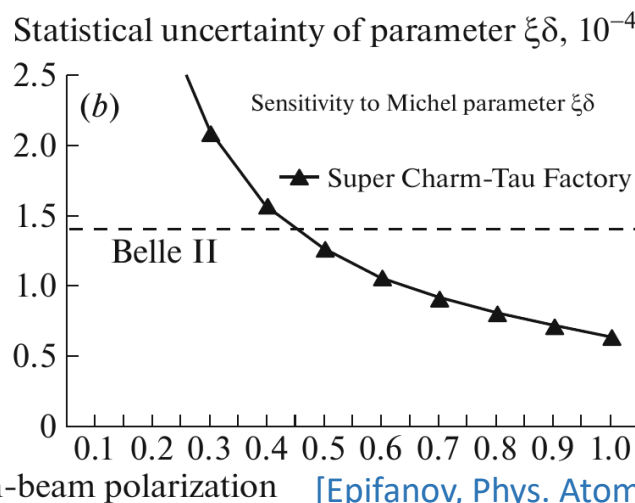
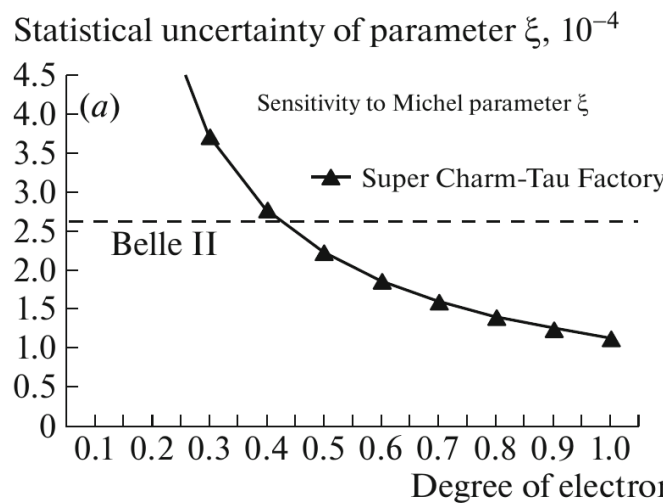
Leptonic τ decays

Michel parameters

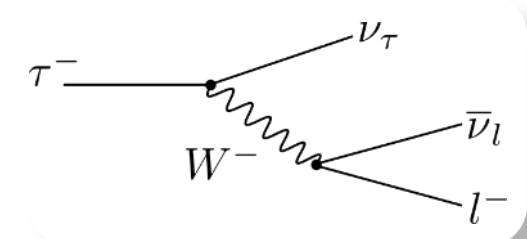
$$\frac{d\Gamma(\tau^\mp)}{d\Omega dx} \propto x(1-x) + \frac{2}{9}\rho(4x^2 - 3x - x_0^2) + \eta x_0(1-x) \mp \frac{1}{3}P_\tau \cos \theta_l \xi \sqrt{x^2 - x_0^2} \left[1 - x + \frac{2}{3}\delta \left(4x - 4 + \sqrt{1 - x_0^2} \right) \right]$$

➤SCT with polarized electrons allows measurement the tau lepton Michel parameters with precision better than that of Belle II

$$x \equiv \frac{E_l}{E_{\max}}, \quad x_0 \equiv \frac{m_l}{E_{\max}}$$



[Epifanov, Phys. Atom. Nucl. 83 (2020) 944]



LFV and CPV with tau

$\tau \rightarrow \mu\gamma$

- Allowed in several BSM scenario, including SUSY, leptoquarks, technicolor, extended Higgs models etc.
- $\mathcal{O}(10^{-9})$ – reachable upper limit at SCT for the branching of $\tau \rightarrow \mu\gamma$.

CP symmetry breaking

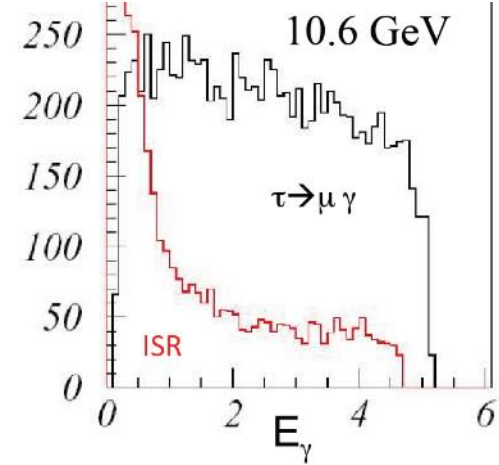
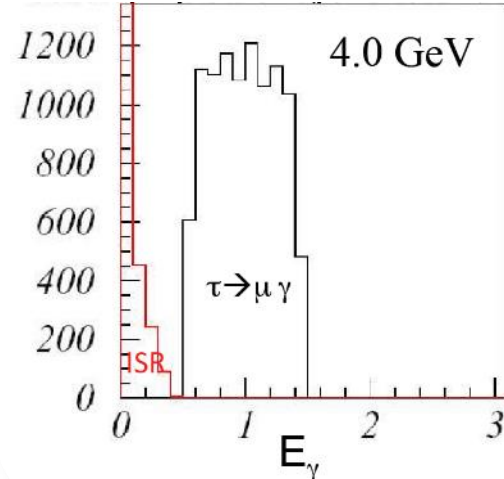
- CPV in tau production

$$J_{EM} \propto F_1 \gamma^\mu + \left(\frac{i}{2m_\tau} F_2 + \gamma^5 F_3 \right) \sigma^{\mu\nu} q_\nu$$

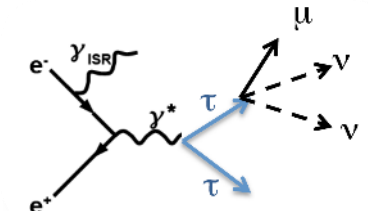
- Current limit: $|d_\tau| \lesssim 10^{-17} e \cdot \text{cm}$
- Tau EDM with polarized electrons [[PRD 51 \(1995\) 5996](#)]:
 $\sigma(d_\tau) \sim 10^{-20} e \cdot \text{cm}$

- CPV in tau decays (e.g., $\tau \rightarrow K\pi\nu_\tau$)

ISR photon background [arXiv:1206.1909 [hep-ex]]



Beam polarization is essential
for these measurements



J/ψ cross section asymmetry

- Interference between the $e^+e^- \rightarrow \gamma^*, Z \rightarrow J/\psi$ processes produces left-right total cross section asymmetry

$$A_{LR} \equiv \frac{\sigma_+ - \sigma_-}{\sigma_+ + \sigma_-} = \frac{3/8 - \sin^2 \theta_{\text{eff}}^c}{2 \sin^2 \theta_{\text{eff}}^c (1 - \sin^2 \theta_{\text{eff}}^c)} \left(\frac{m_{J/\psi}}{m_Z} \right)^2 P_e \approx 4.7 \times 10^{-4} P_e$$

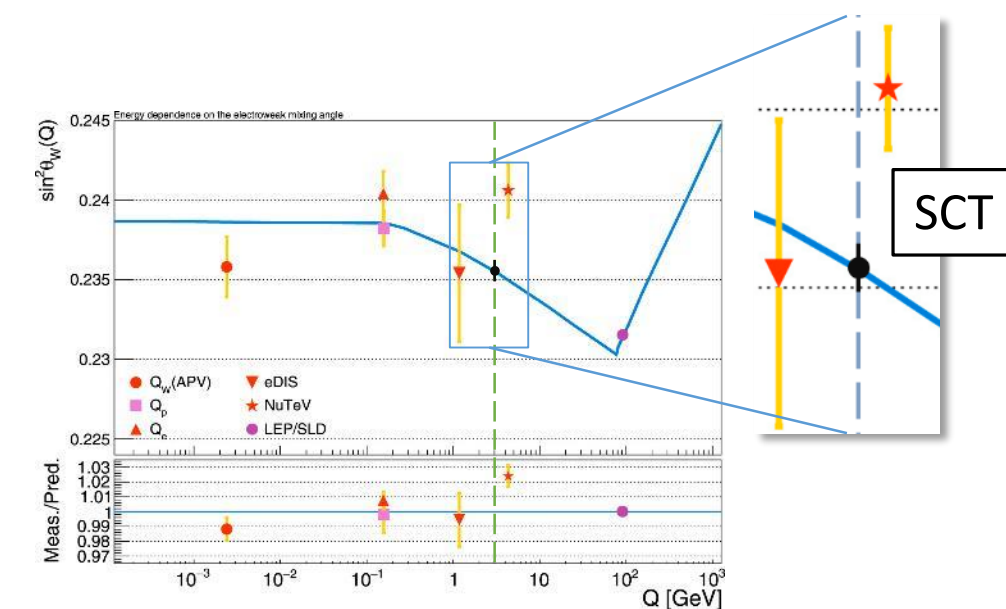
- σ_+ (σ_-) is the total $e^+e^- \rightarrow J/\psi$ cross section for right- (left-)handed electrons
- P_e is the average electrons polarization, $P_e < 1$

- Statistical precision with a one-year data set:

$$\frac{\sigma(\sin^2 \theta_{\text{eff}}^c)}{\sin^2 \theta_{\text{eff}}^c} \approx 0.3\%, \quad \sigma(\sin^2 \theta_{\text{eff}}^c) \approx 5 \times 10^{-4}$$

- It tests weak interaction of the charm quark

- An opportunity to observe deviation of the $\sin^2 \theta_{\text{eff}}^c$ from its value at Z peak (test of the EW model)



JHEP 2020, 76 (2020)

Physics program: 2022 update

Оглавление

Введение

1 Чармопий (К.Тоддичин)	11
1.1 Составление ниже порога $D\bar{D}$	12
1.2 Изучение экзотических состояний чармона	14
1.2.1 X-состояния	14
1.2.2 Y-состояния	16
1.2.3 Z ₀ -состояния	18
2 Спектроскопия состояний из легких квarks (М.Ачисов)	21
2.1 Легкие кварты в квантовой хромодинамике	22
2.2 Модель конституентных квартов	23
2.3 Экзотические состояния	26
2.3.1 Глюонный	26
2.3.2 Гифры	28
2.3.3 Многоцентровые состояния	28
3 Физика D-мезонов (В.Боробин)	30
3.1 Введение	30
3.2 Отбор D-мезонов в горячем эксперименте	33
3.3 Статистическая D-модель	35
3.4 Изучение абсолютной вероятности распадов	39
3.5 Летонные и полуплетонные распады D-мезонов	41
3.6 Редкие и запрещенные распады D-мезонов	45
3.7 Симметрии в системе нейтральных D-мезонов	50
3.7.1 Введение	50
3.7.2 Распады некогерентных состояний	53
3.7.3 Распады когерентных пар D	54
3.7.4 Анализ распада $D \rightarrow K_S^0 \pi^+ \pi^-$	55
3.8 Изучение сильных флюктуаций распада D-мезонов	59
3.9 Измерение сильных флюктуаций в распадах очарованных адронов внейтральном касио (В.Попов, П.Паслов)	64
3.9.1 Измерение сильных флюктуаций с использованием полулетоновых распадов нейтральных касио	66
3.9.2 Измерение сильных флюктуаций с использованием СР-составного конечного состояния нейтрального касио	67
3.9.3 Оценка потенциальной точности измерения сильных флюктуаций	68

6

4 Очарованные барионы (Т.Углов)	70
4.1 Изменение форм-факторов очарованных барионов	71
4.2 Поиск СР-нарушений в распадах очарованных барионов	73
5 Физика τ-лектона (Д.Ениеванов)	75
5.1 Введение	75
5.2 Свойства τ-лектона	76
5.2.1 Проверка лектонной универсальности	76
5.2.2 Масса τ-лектона	77
5.2.3 Время жизни τ-лектона	78
5.2.4 Электрический и магнитный дипольные моменты τ-лектона	79
5.3 Летонные распады τ-лектона	81
5.3.1 Сложная проблемная структура заряженного слабого взаимодействия	81
5.3.2 Особенности летонных распадов τ-лектона	83
5.3.3 Радиационные летонные распады τ-лектона	84
5.3.4 Платитонные летонные распады τ-лектона	86
5.4 Адронные распады τ-лектона	89
5.4.1 $\tau \rightarrow P \nu_\tau$, ($P = \pi, K$)	89
5.4.2 $\tau \rightarrow P' \nu_\tau \gamma$ и $\tau^+ \rightarrow P' \ell^+ \ell^- \nu_\tau$, ($P = \pi, K; \ell = e, \mu$)	90
5.4.3 $\tau^+ \rightarrow \pi^+ \pi^0 \nu_\tau$	91
5.4.4 Поиск токов второго класса в адровых распадах τ-лектона	92
5.4.5 Адронные распады τ ⁺ в состоянии с квазим в конечном состоянии	94
5.5 СР-нарушение в распадах τ-лектона	97
5.6 Нарушение лектонного квазим в распадах τ-лектона	101
5.7 Измерение параметров Мишеля в распадах $\tau^+ \rightarrow \mu^+ \nu_\mu \beta_1$ с распадами мюона на зету (Д.Бордов)	102
6 Измерение сечения $e^+e^- \rightarrow \text{адроны}$	106
7 Двухфотонная физика (В.Дружинин)	110
8 Поиск Новой физики в распадах σ-кварка	111
8.1 Переходы $c \rightarrow (s, d) l^+ l^-$	112
8.2 Переходы $c \rightarrow u \bar{d}^+ \Gamma$, $c \rightarrow u \bar{d}$, $c \rightarrow u \bar{u} \Gamma$	117
Заключение	121

7

➤ 2021: ≈ 40 pages

➤ 2022: ≈ 120 pages

➤ In Russian

➤ Editors:

- G.Pakhlova (LPI)
- A.Bondar (BINP)

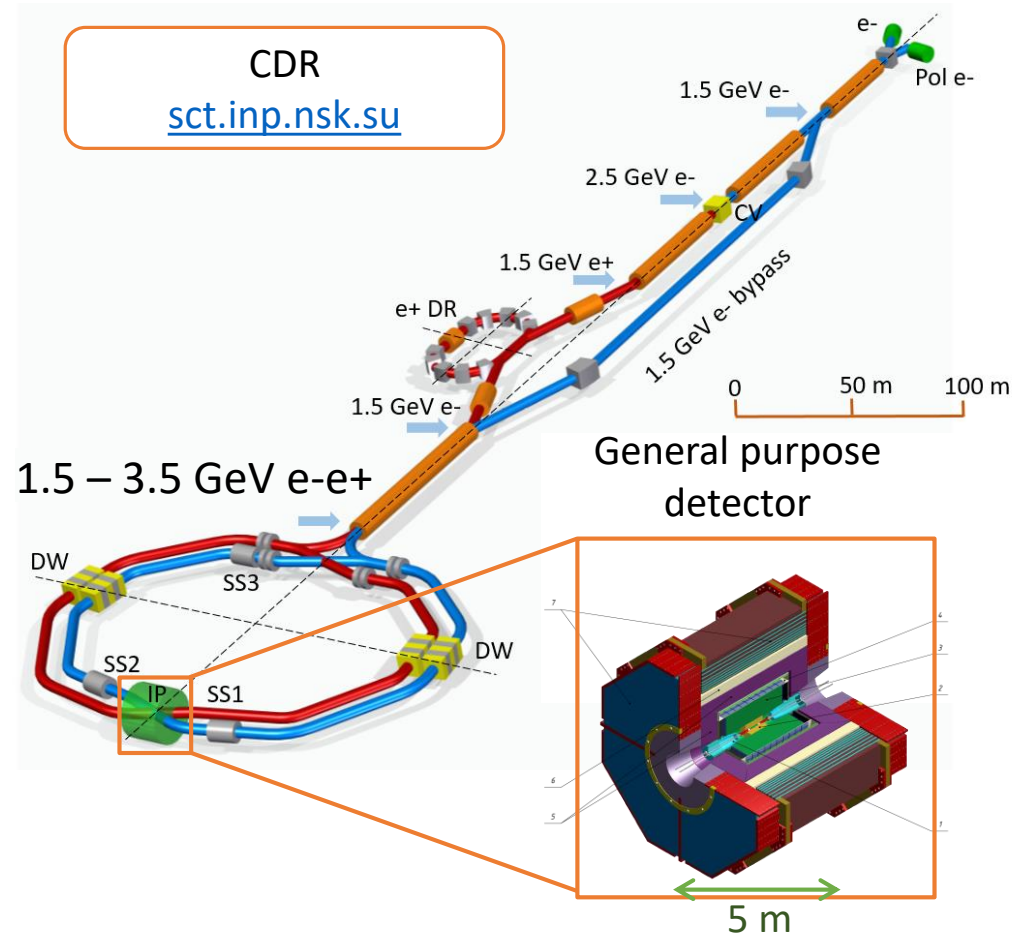
Shorter (extracted) version
prepared as a white paper for
Snowmass

<http://sct.inp.nsk.su>

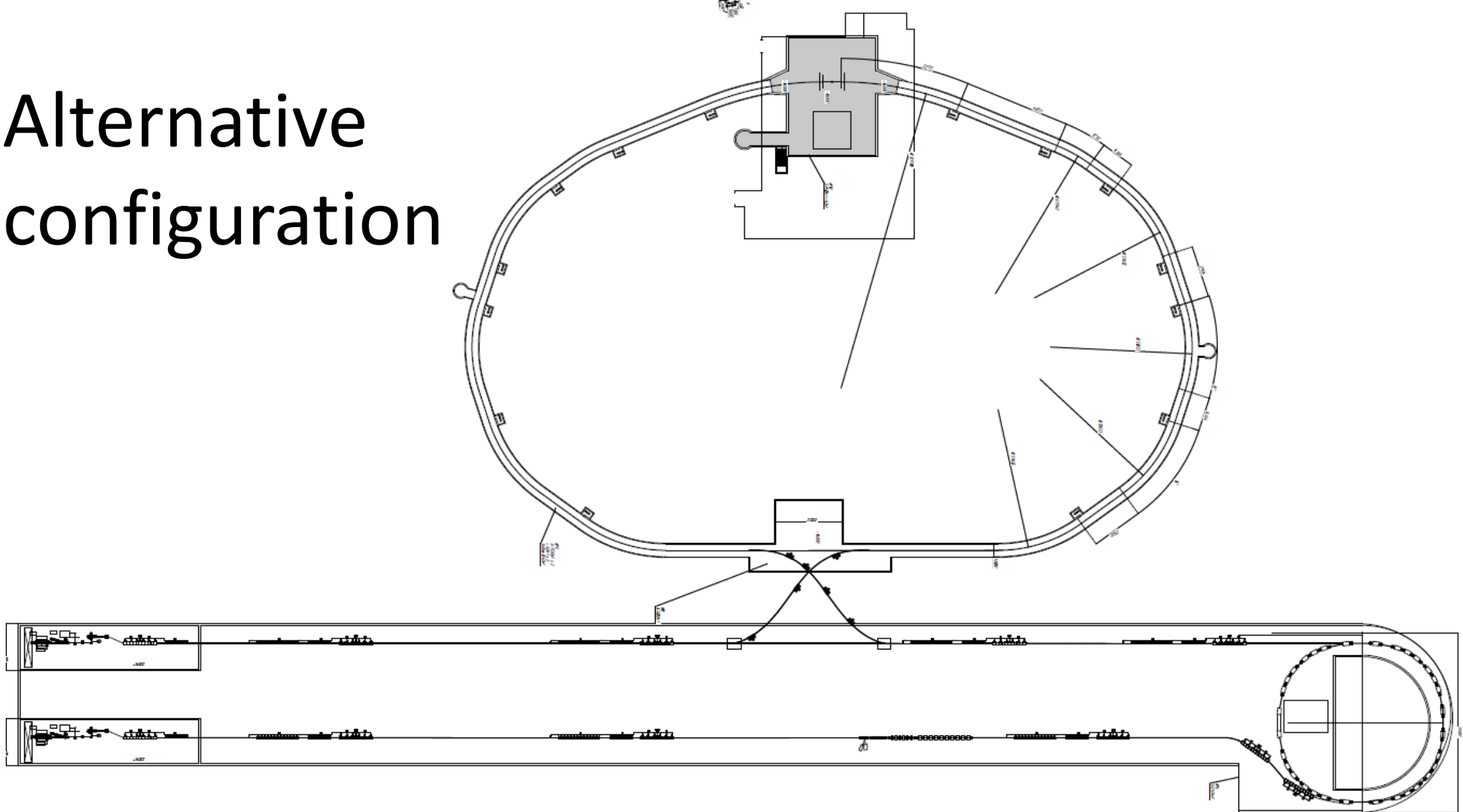
Collider

Super charm-tau factory

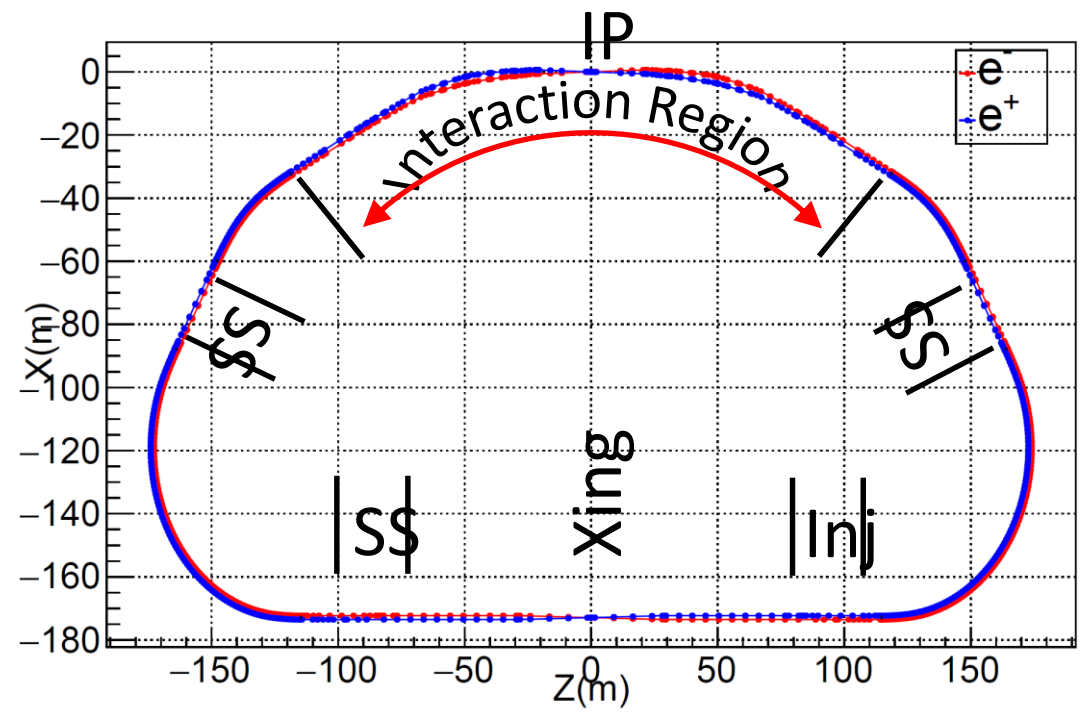
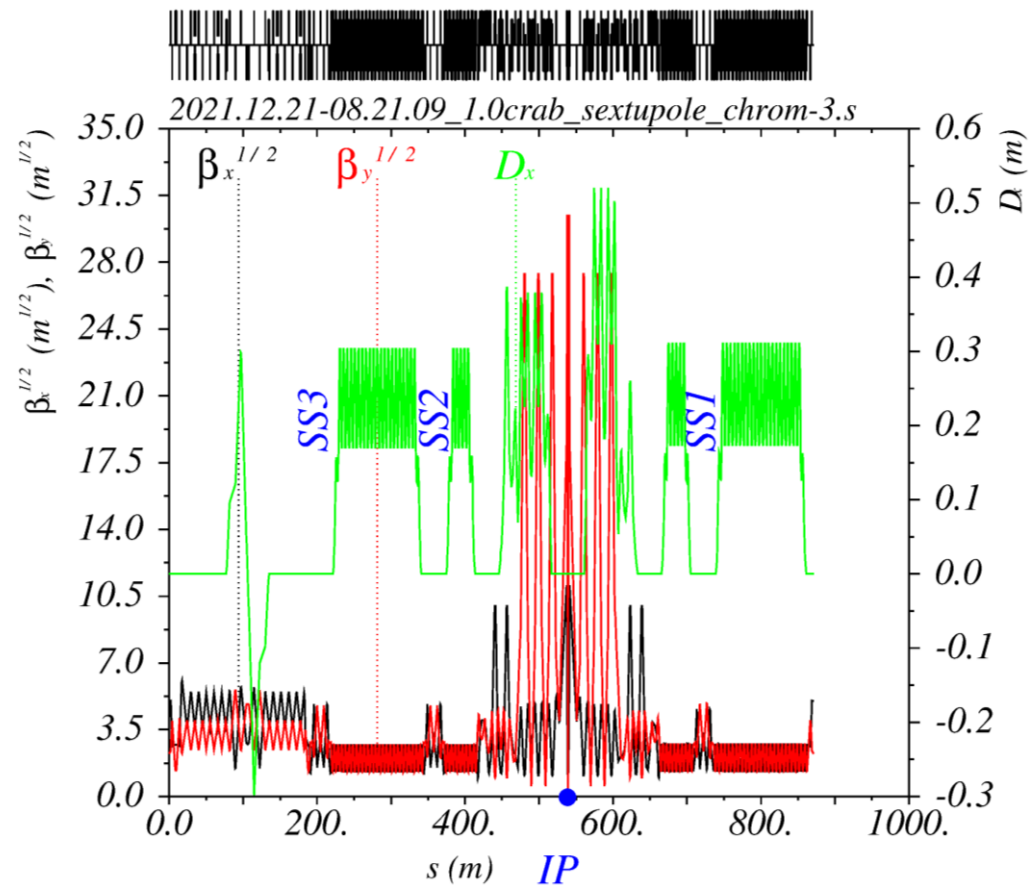
- Super charm-tau factory is e^+e^- collider, dedicated to precision study of properties of charm-quark, tau-lepton, study of strong interactions, search of BSM physics
 - Beam energy from 1.5 (1.0) to 3.5 GeV
 - Luminosity $\mathcal{L} = 10^{35} \text{ cm}^{-2}\text{c}^{-1}$ @ 2 GeV
 - Longitudinally polarized electron beam
 - Experiments will be conducted using state-of-the-art general purpose detector
 - Tracking (including low p_t)
 - Calorimetry (high resolution, fast, π^0/γ sep.)
 - Particle ID ($\mu/\pi/K/p$ up to 1.5 GeV/c)



Alternative configuration



Lattice and layout (2021)



Design parameters (2021)

- Design parameters meet the luminosity requirements
- Similar parameters have been achieved at other colliders
- Dynamic aperture was not taken into account

The key problem now is to find configuration with sufficient dynamic aperture

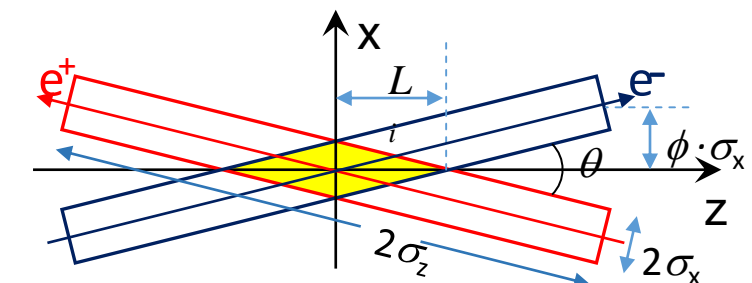
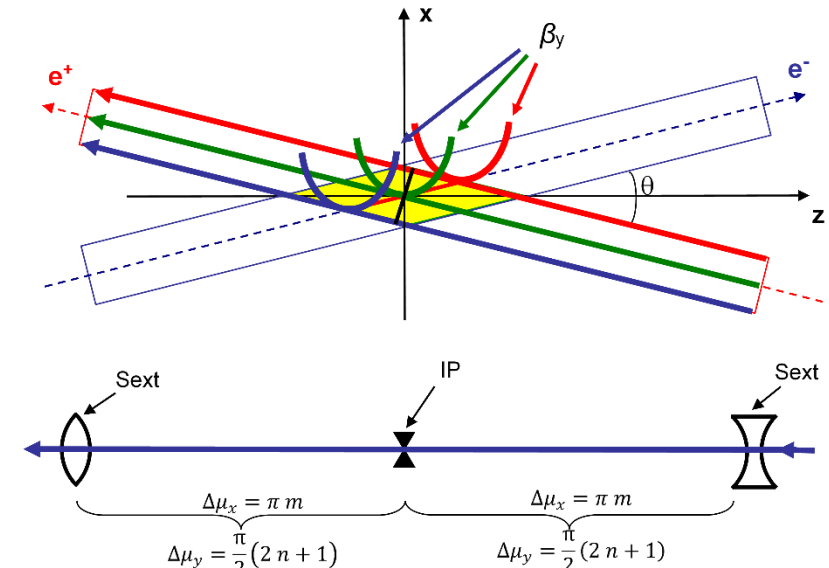
$E[\text{MeV}]$	1500	2000	2500	3000	3500	
$\Pi[\text{m}]$			870.949			
$f_{RF}[\text{MHz}]$			350			
$2\theta[\text{mrad}]$			60			
$\epsilon_y/\epsilon_x[\%]$			0.5	SuperKEKB 03.12.2019 $\beta_y^* = 1 \text{ mm}$		
$\beta_x^*/\beta_y^* [\text{mm}]$		100/1				
$I[\text{A}]$	2	2	2	2	2	
$N_{e/bunch} \times 10^{-10}$	9	8	7	8	PEPII: $I(e+) = 3.2 \text{ A}$ PEPII DAFNE : $I(e-) = 2.45 \text{ A}$	
N_B	420	472	540	47		
$U_0[\text{keV}]$	115.6	294	516	845	1314	
$V_{RF}[\text{kV}]$	1500	2300	3000	3500	4500	
v_s	0.0152	0.0162	0.0165	0.0162	0.0168	
$\delta_{RF}[\%]$	1.9	2	2	1.8	1.8	
$\sigma_e \times 10^3 \text{ (SR/IBS+WG)}$	0.28/1.1	0.37/1.1	0.5/1.1	0.6/1.2	0.7/1.5	
$\sigma_s[\text{mm}] \text{ (SR/IBS+WG)}$	3.6/14	5/14	6/14	7/15	8/15	
$\epsilon_x[\text{nm}] \text{ (SR/IBS+WG)}$	2.3/7.3	4/4.9	6/4.3	SuperKEKB: $L = 4.7 \times 10^{34}$		
$L_{HG} \times 10^{-25} (\text{cm}^{-2} \text{s}^{-1})$	0.87	1.1	1	1	1	
ξ_x/ξ_y	0.008/0.17	0.005/0.14	0.004/0.1	0.003/0.09	0.003/0.07	
$\tau_{\text{Luminosity}} [\text{s}]$	2400	2100	2300	2300	2400	

To remind: Crab waist (P.Raimondi 2006)

Large Piwinski angle: $\phi = \frac{\sigma_z}{\sigma_x} \tan\left(\frac{\theta}{2}\right)$

1. Transverse beam separation in parasitic IPs
 - distance between bunches is not limited by beam-beam
2. Interaction area length $L_i \ll \sigma_z$
 - $\beta_y^* \approx L_i \ll \sigma_z$ no hour-glass
3. CRAB waist (CRAB sextupoles) suppresses betatron and synchro-betatron resonances
 - $\xi_y \sim 0.2$

But CRAB sextupoles introduce large nonlinearity, which reduces dynamic aperture, for off-momentum particles



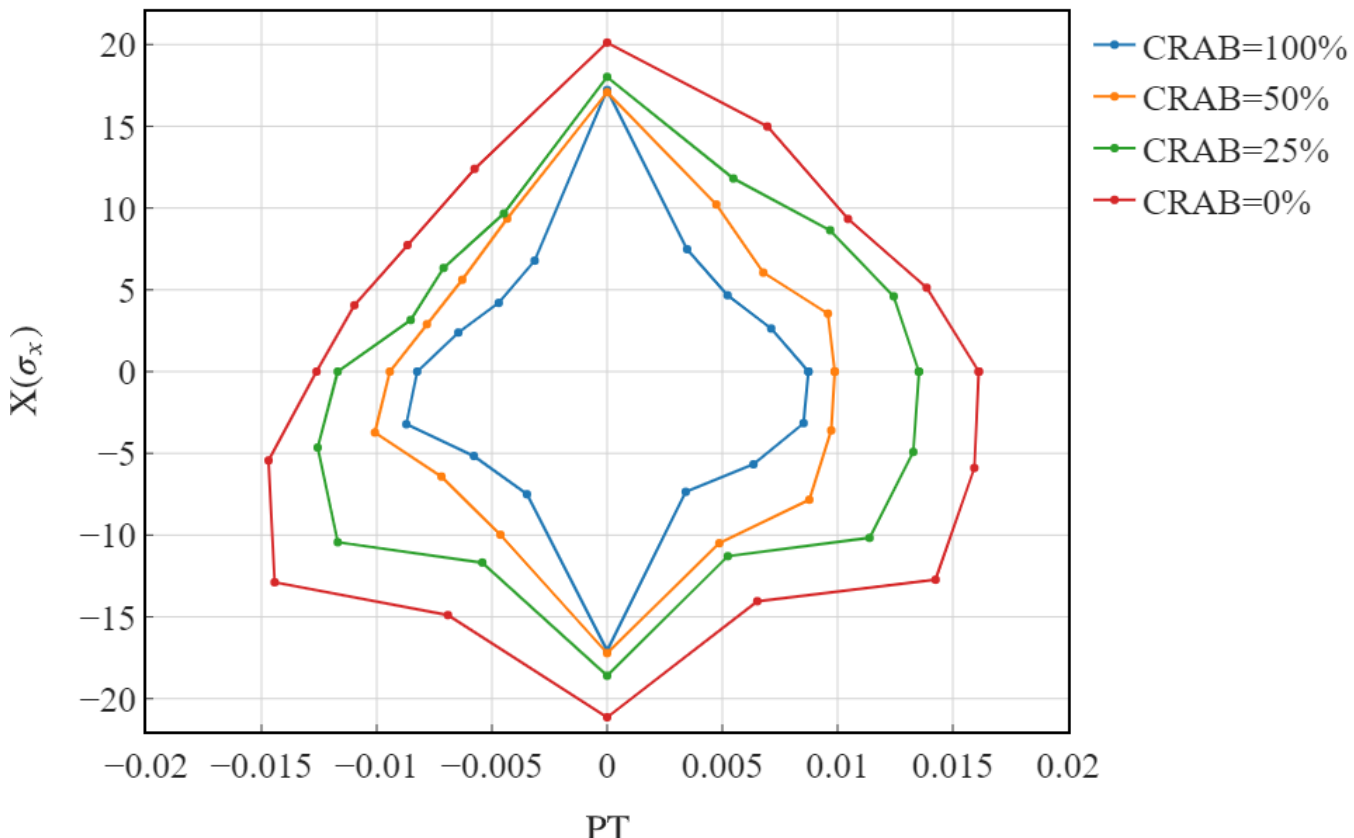
CRAB sextupole influence on 6d DA, E=1.5 ΓΞB, IP1

“Interaction region 1” configuration

- Off momentum dynamic aperture with CRAB ON is insufficient at 1.5-2.5 GeV to provide necessary Touschek lifetime

$E = 1.5$ GeV	CRAB 0%	CRAB 25%	CRAB 50%	CRAB 100%
$N_{part},$ $\times 10^{-10}$	9	4	1.6	0.6
$\tau_{Touschek}(s)$	265	255	240	230
$L(cm^{-2}s^{-1})$ $\times 10^{-34}$	9.9	5.4	1.2	0.19

$$6d\text{-DA}, y_0 = \sigma_y, \sigma_x = 4.72e - 04, \sigma_\delta = 1.12e - 03$$



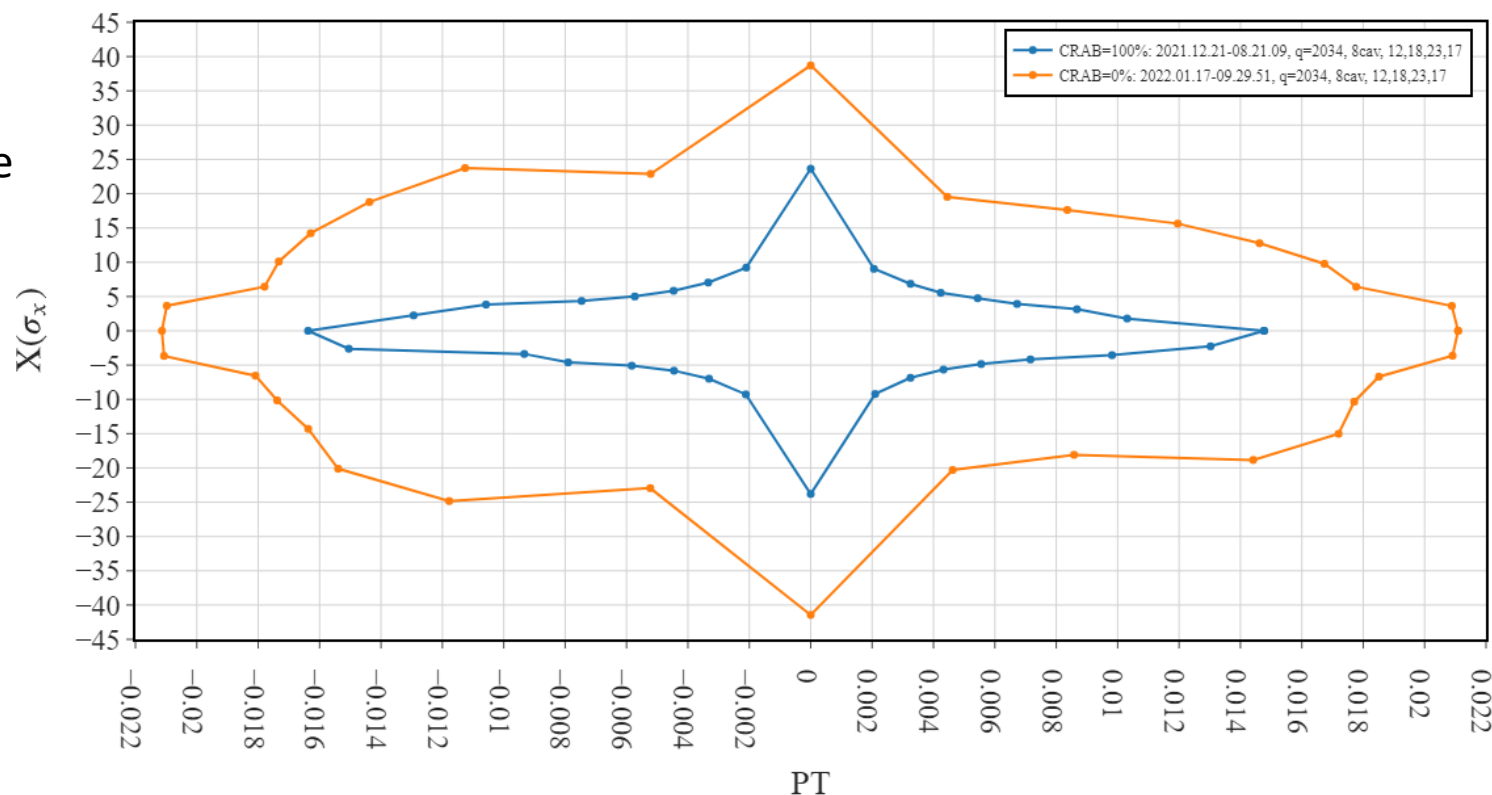
Touschek lifetime with CRAB ON and OFF at 2 GeV, IP3

“Interaction region 3” configuration

- Placing CRAB sextupoles closer to IP gives larger energy aperture
- But still not sufficient for Touschek lifetime at 1.5, 2 GeV with CRAB sextupole 100%

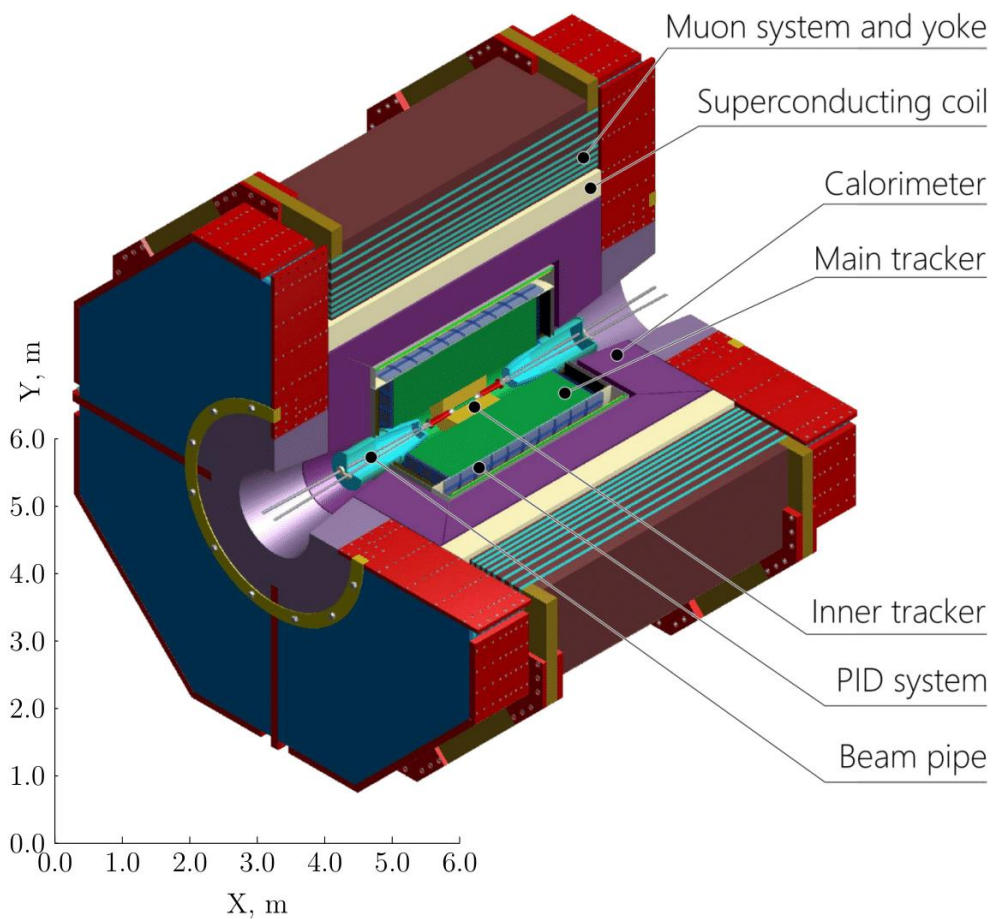
	CRAB OFF	CRAB ON
$\tau_T(s)$	740	108
$N_p(10^{10})$	2.7	2.7

6d-DA, $y_0 = \sigma_y$, $\sigma_x = 3.50e - 04m$, $\sigma_e = 1.14e - 03$, 2 GeV



Detector

Detector concept



Momentum resolution $\sigma_p/p \leq 0.4\%$ at 1 GeV

Very symmetric and hermetic

Able to detect soft tracks ($p_t \geq 50 \text{ MeV}/c$)

- Inner tracker should be able to handle $10^4 \text{ tracks/cm}^2\text{s}$

Very good particle identification: $e/\mu/\pi/K$

- π/K in the whole energy range, e.g. for $D\bar{D}$ mixing
- μ/π up to 1.5 GeV, e.g. for $\tau \rightarrow \mu\gamma$ search
- dE/dx better than 7%

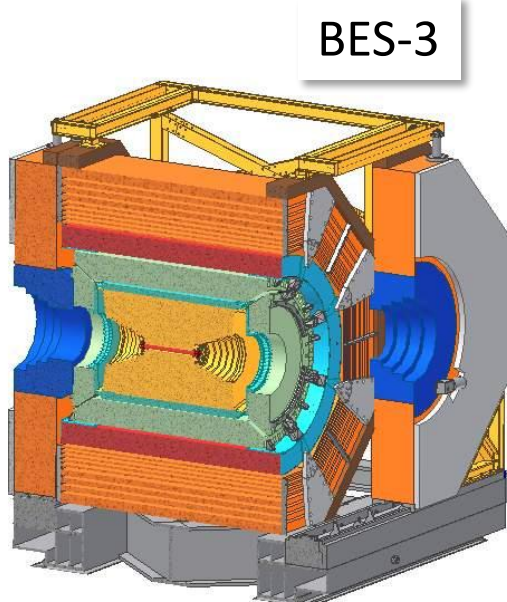
Able to detect γ from 10 MeV to 3.5 GeV, good π^0/γ separation

- Calorimeter energy resolution $\sigma_E/E \leq 1.8\%$ at 1 GeV
- Calorimeter time resolution $\sigma_t \leq 1 \text{ ns}$

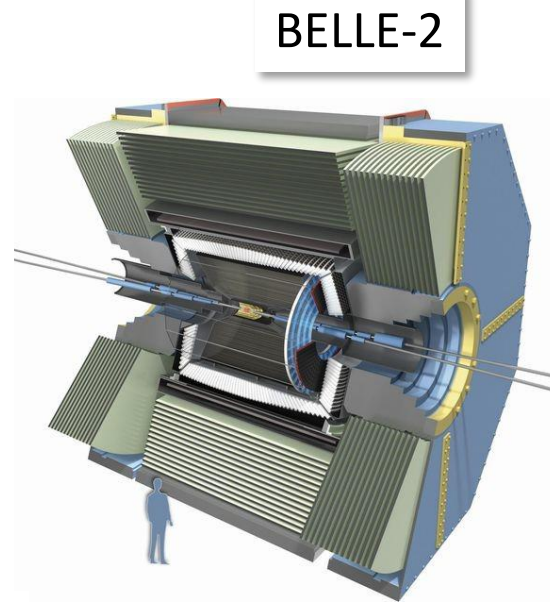
Efficient “soft” trigger

Ability to operate at high luminosity, up to 300 kHz at J/ψ

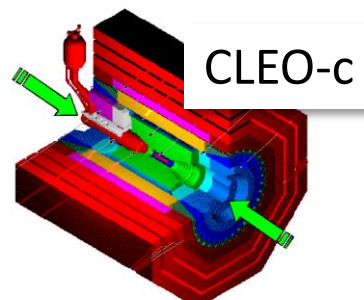
Brothers, sisters and cousins...



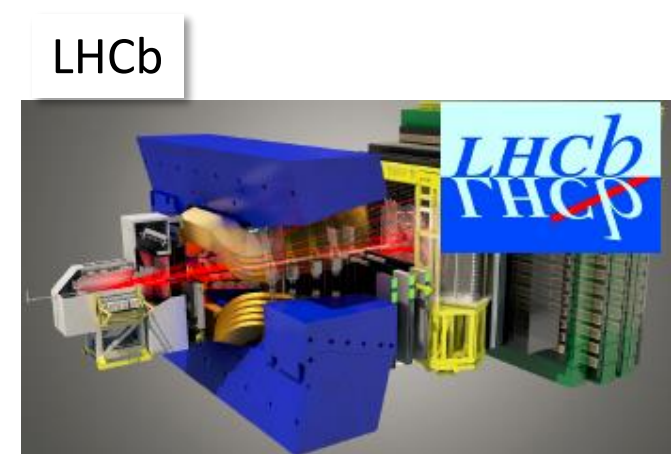
Very similar
1% luminosity



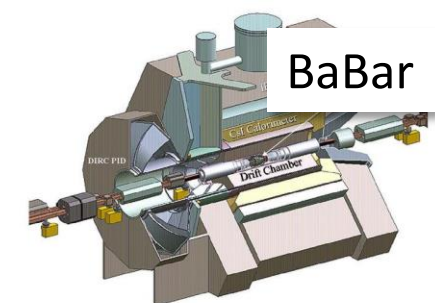
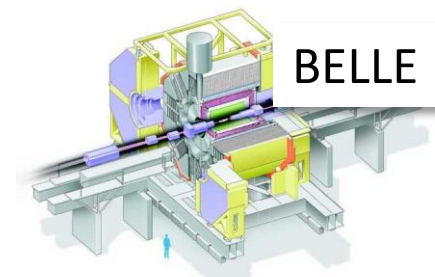
Super B-factory (10.58 GeV)
5-10x luminosity



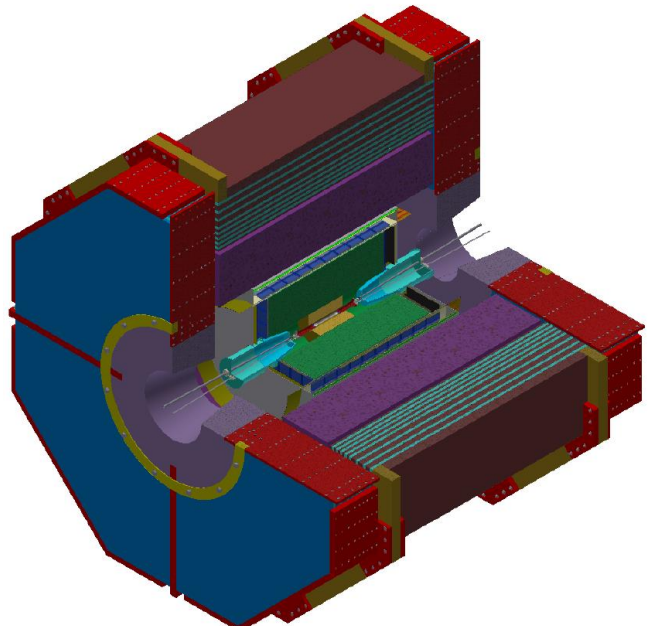
← Previous generation →



pp collisions



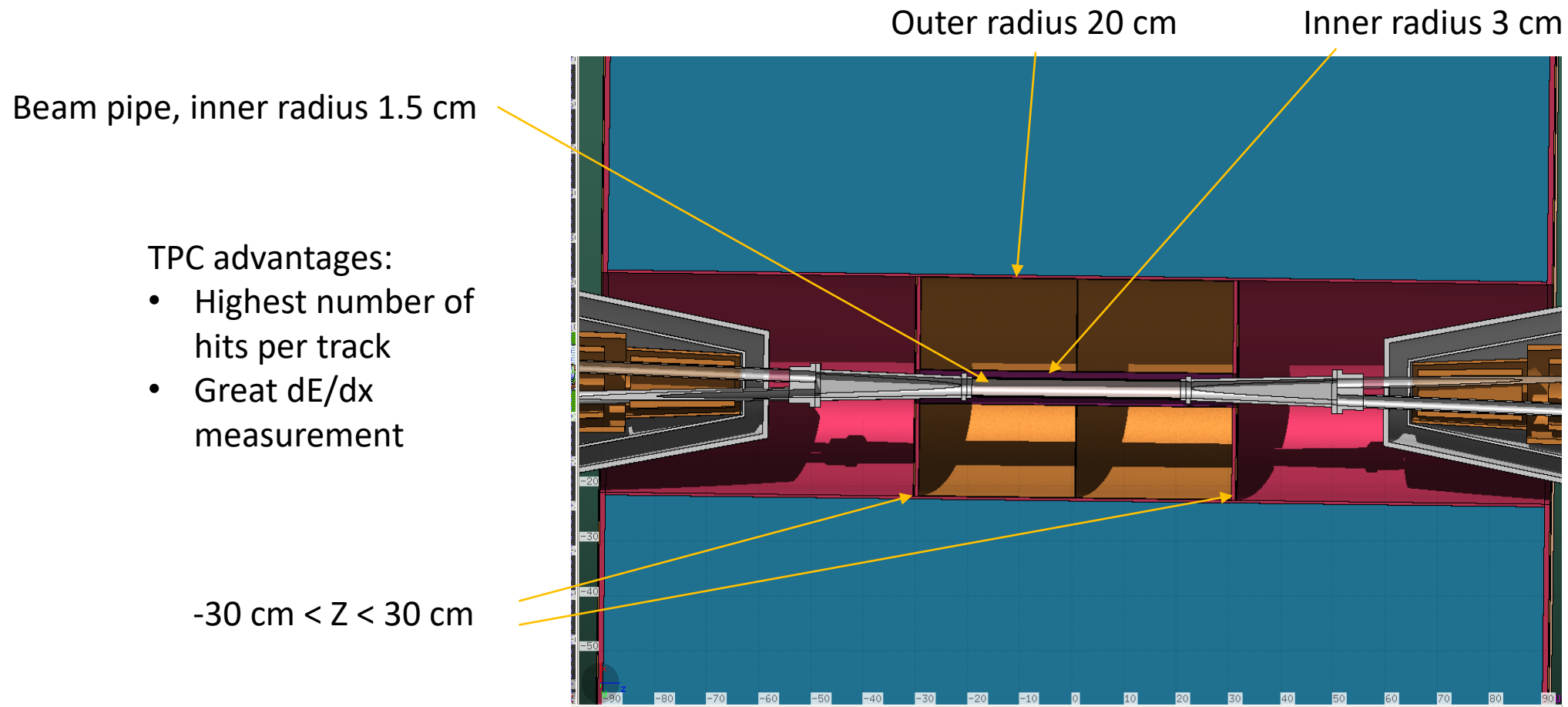
On-going R&Ds for detector



- Inner tracker
 - Time projection chamber (TPC) option by [BINP](#)
 - Cylindrical μ RWELL option by [INFN \(LNF, Ferrara\)](#)*
- Main tracker
 - Drift chamber option by [BINP](#)
 - Ultra thin DC (TraPID) option by [INFN \(Lecce, Bari\)](#)*
- PID system
 - FARICH option by [BINP](#)
 - FDIRC options by [Giessen University](#)*
- Electromagnetic calorimeter – [BINP](#)
- Muon system – [Lebedev Physics Institute \(LPI\)](#)
- Magnet – [BINP](#)
- Detector software – the AURORA framework released in 2021

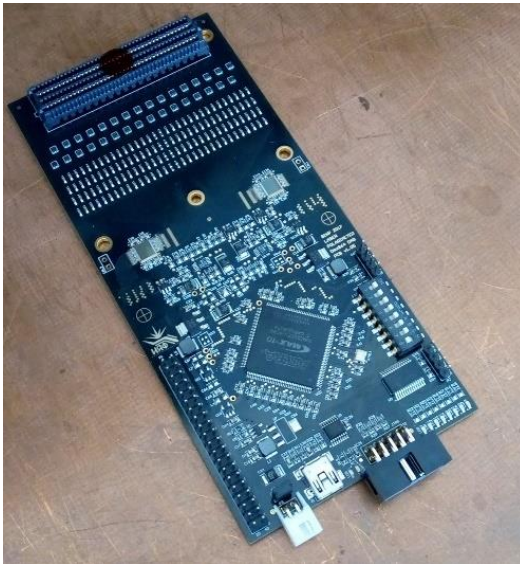
* Before spring 2022

Inner Tracker: TPC

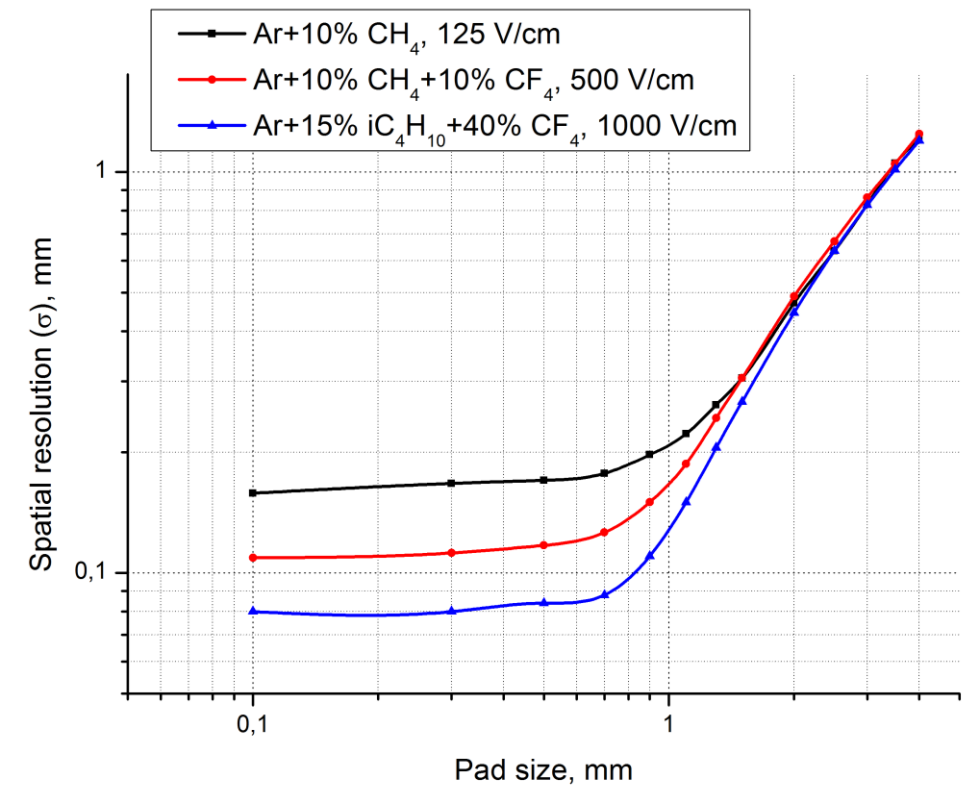


Inner Tracker: simulations and prototyping

The prototype is being built at BINP



Simulation of spatial resolution in TPC



Inner Tracker: C-mRWELL

The c- μ RWELL option for IT was proposed by G.Bencivenni (INFN)

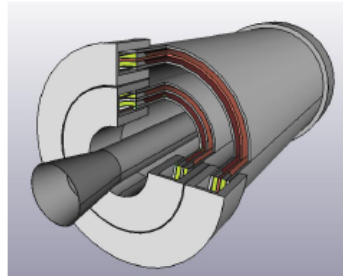


The Cylindrical u-RWELL



The two schemes under study are both based on a **B2B layout** (a double radial TPC – with a central cathode), characterized by low material budget and modular roof-tile shaped active device

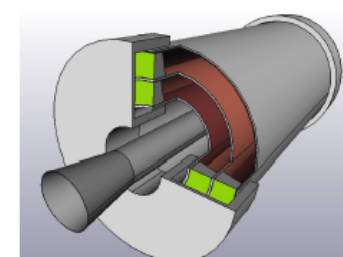
"2 - B2B small drift gap" cylindrical detector



N.2 small gap B2B C+layers \rightarrow 1.72% X0
2 \times 1 cm gas gap/B2B device
4 cm global sampling gas

"1 - B2B large drift gap" cylindrical detector

micro-TPC readout mode allowing space resolution of O(100 μ m) for inclined tracks (on the radial view)



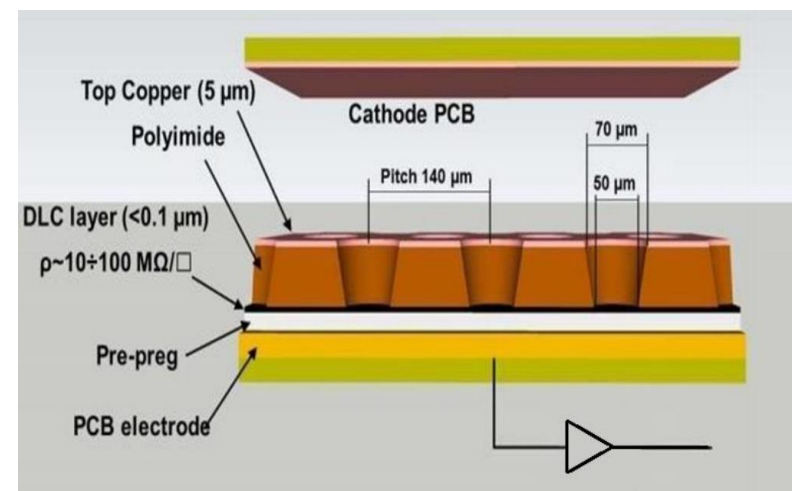
- N.1 large gap B2B C+layers \rightarrow 0.86% X0
- 2 \times 1 cm gas gap/B2B device
- 10 cm global sampling gas

1.46 % X0

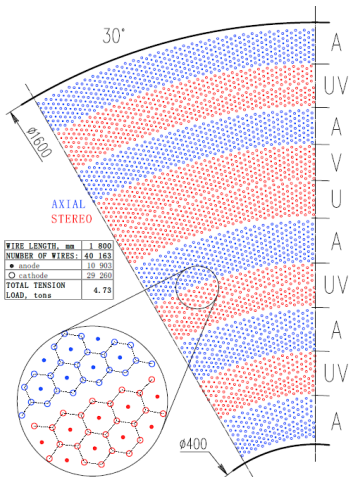
Further material budget reduction by using:

- high module FR4
- low resistivity DLC cathode
- aluminum Faraday-Cage/shielding

0.75 % X0

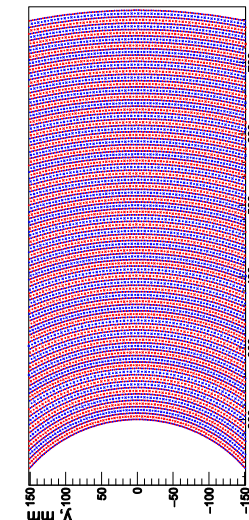


Drift chamber



Measurement of momentum and dE/dx (PID)

- Spatial resolution $\sim 100 \mu$
- Small cell
- Minimal material (reduce MS)
- Approximate size: $\varnothing (400-1600) \times 1800$ mm



“Traditional” option BINP

Babar, BES-3, Belle-2

Axial and stereo superlayers

Traditional dE/dx

Feed-through wiring

“Beyond-traditional” option INFN

KLOE, MEG-2, IDEA

Full stereo

dE/dx by cluster counting

Robotic wiring

Drift chamber: “traditional” option (BINP)

~40000 wires

- 11k sensitive, W-Rh(Au)
- 29k field, Al(Au)

Hexagonal cell, 6.3-7.5 mm

41 layers

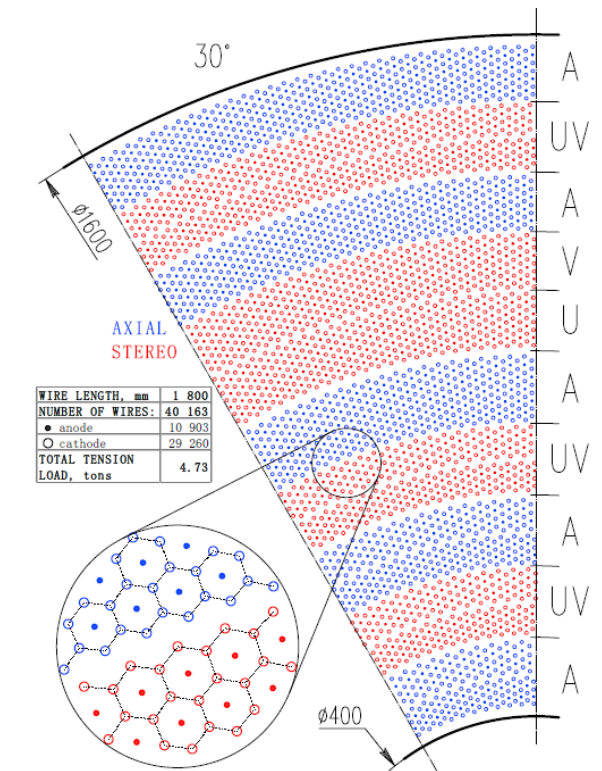
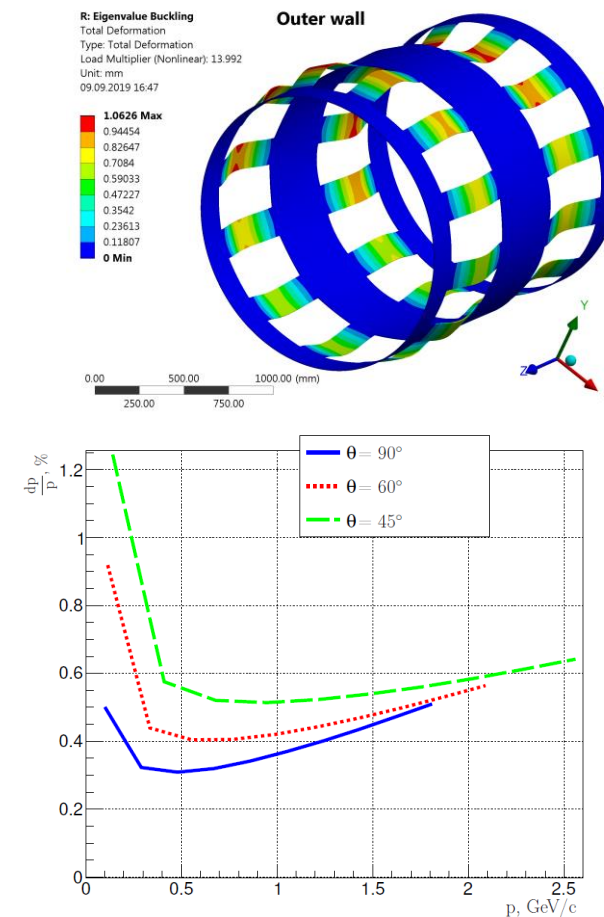
60% He + 40% C₃H₈

330 ns drift time (1.5 T)

$$\frac{\sigma_{p_t}}{p_t} \approx \sqrt{0.21\%^2 p_t^2 + 0.31\%^2}$$

≈0.4% at 1 GeV

$$\frac{\sigma_{dE/dx}}{dE/dx} \approx 6.9\%$$



I.Yu.Basok et al., NIM A1009 (2021) 165490

Drift chamber: TraPid option (INFN)

~141000 wires

- 23k sensitive, W
- 117k field, Al (\rightarrow C)

Square cell, 7.2-9.1 mm

Full stereo

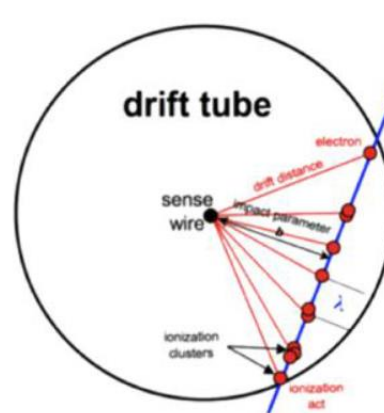
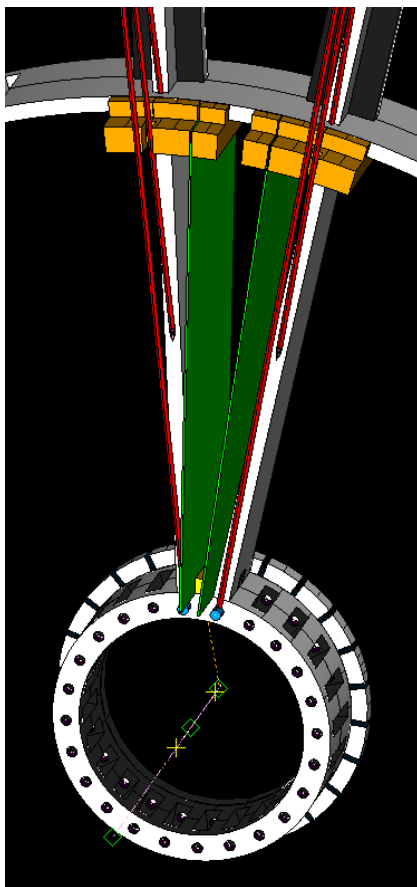
64 layers

90% He + 10% iC₄H₁₀

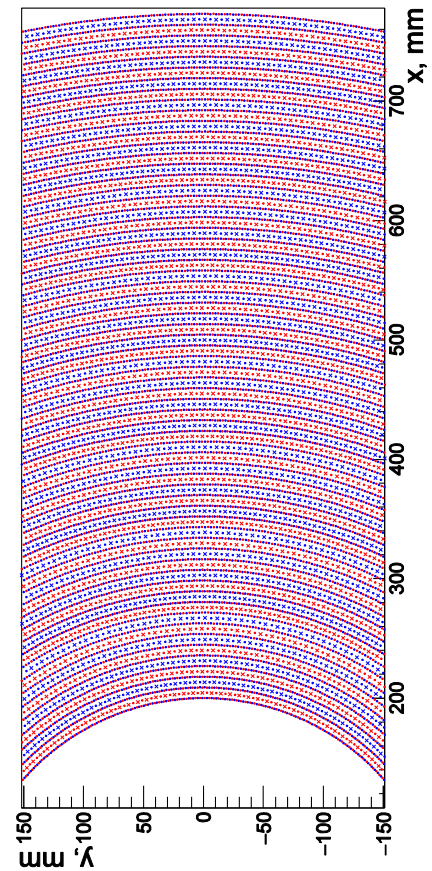
$$\frac{\sigma_{p_t}}{p_t} \approx \sqrt{0.078\%^2 p_t^2 + 0.18\%^2}$$

$\approx 0.2\%$ at 1 GeV

$$\frac{\sigma_{dN/dx}}{dN/dx} \approx 3.6\%$$

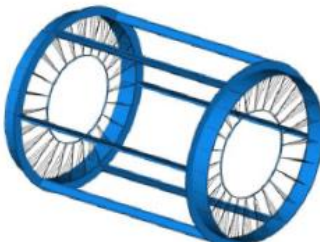


Measurement of individual clusters improves time and dE/dx resolution



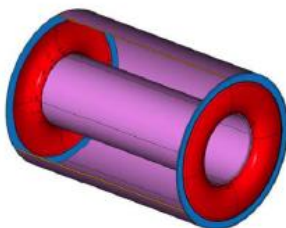
MEG-2 drift chamber

- Separation of the wire anchoring function from the mechanical and wire containment



Wire support

Wire cage structure not subject to differential pressure can be light and feed-through-less.



Gas containment

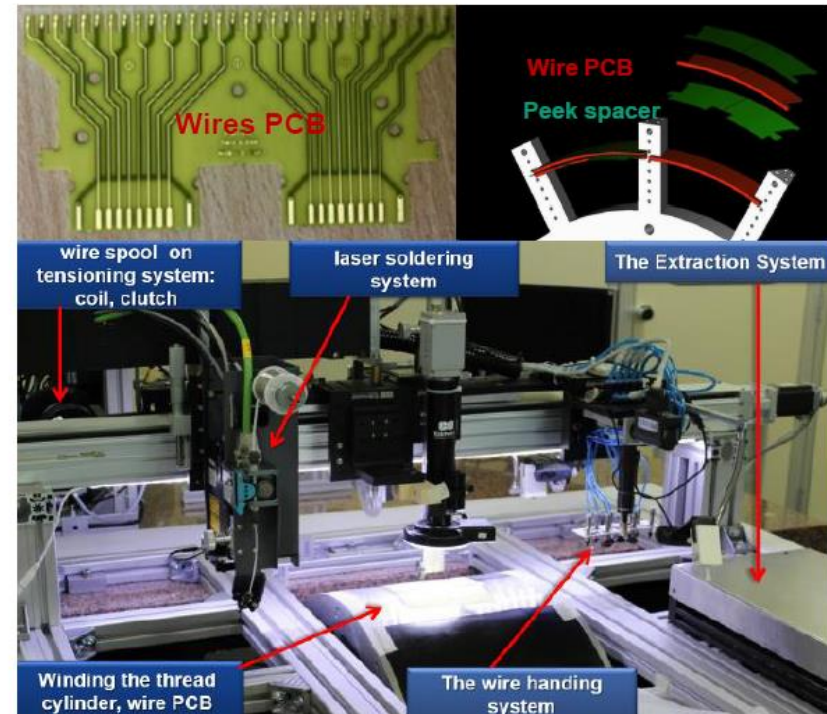
Gas envelope can freely deform without affecting the internal wire position and tension.

- Wire PCB

The high wires density (12 wires/cm^2) imposes the use of **wires PCBs** where the wires are accurately positioned and strung at the correct mechanical tension.

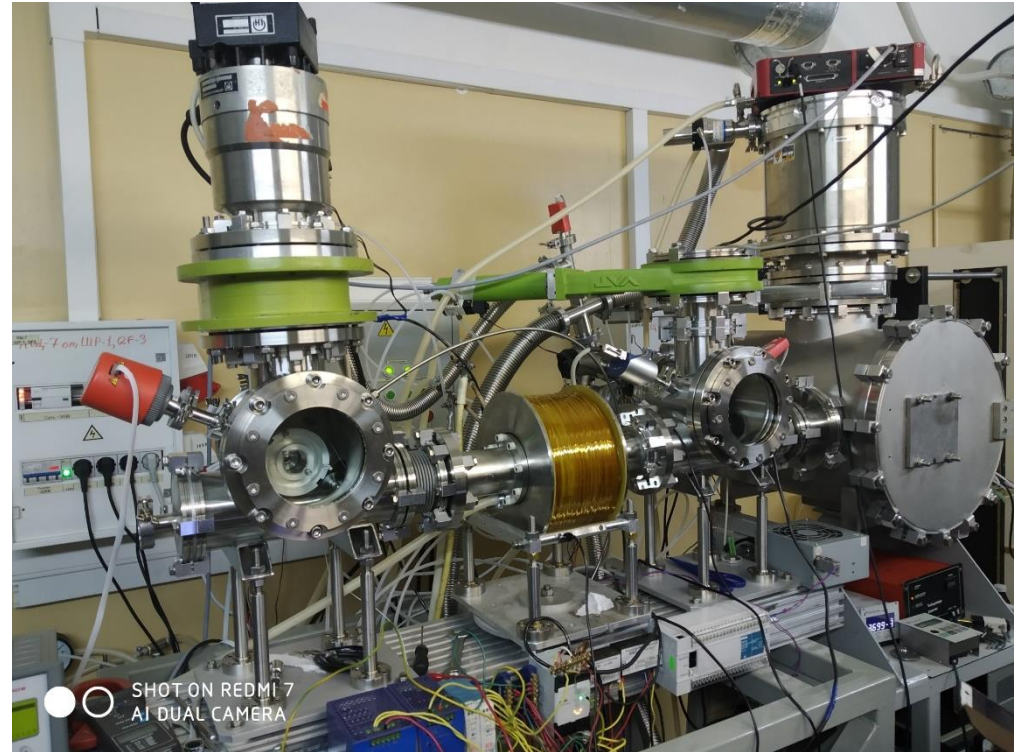
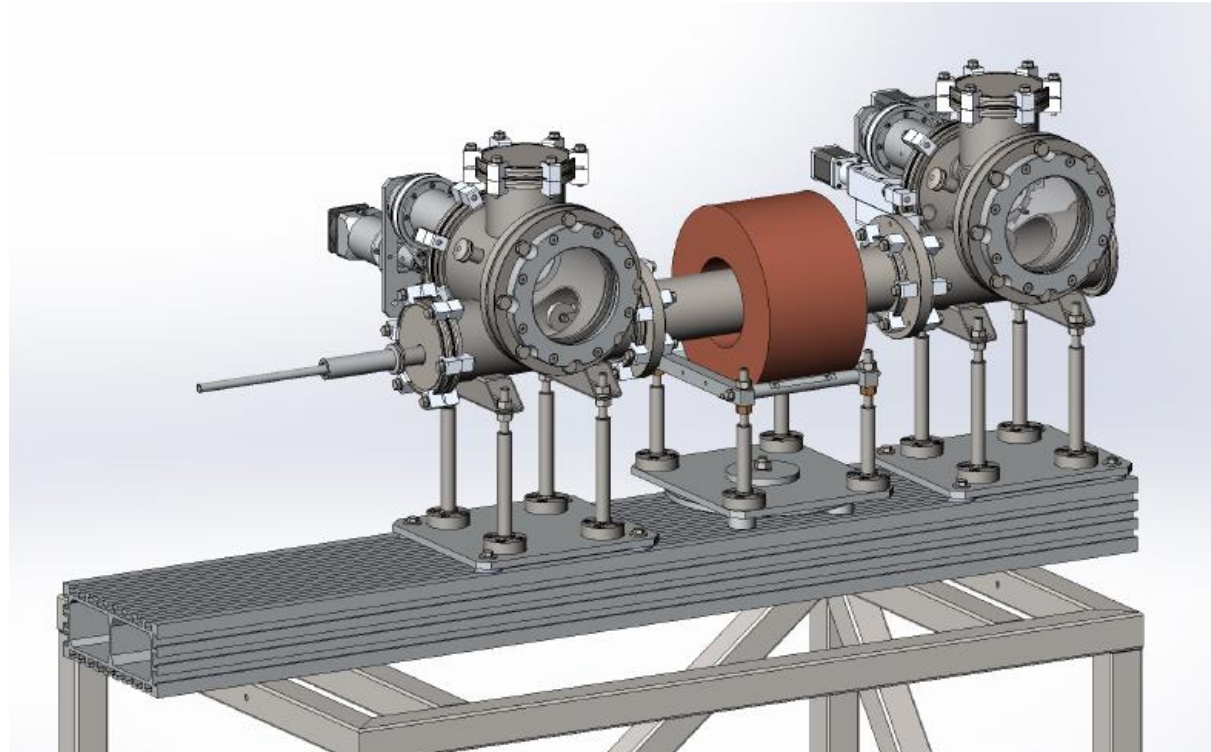
- Wiring robot

Stringent requirements on the precision of wire position and on the uniformity of the wire mechanical tension impose the use of an automatic system (Wiring Robot), to operate the wiring procedures.



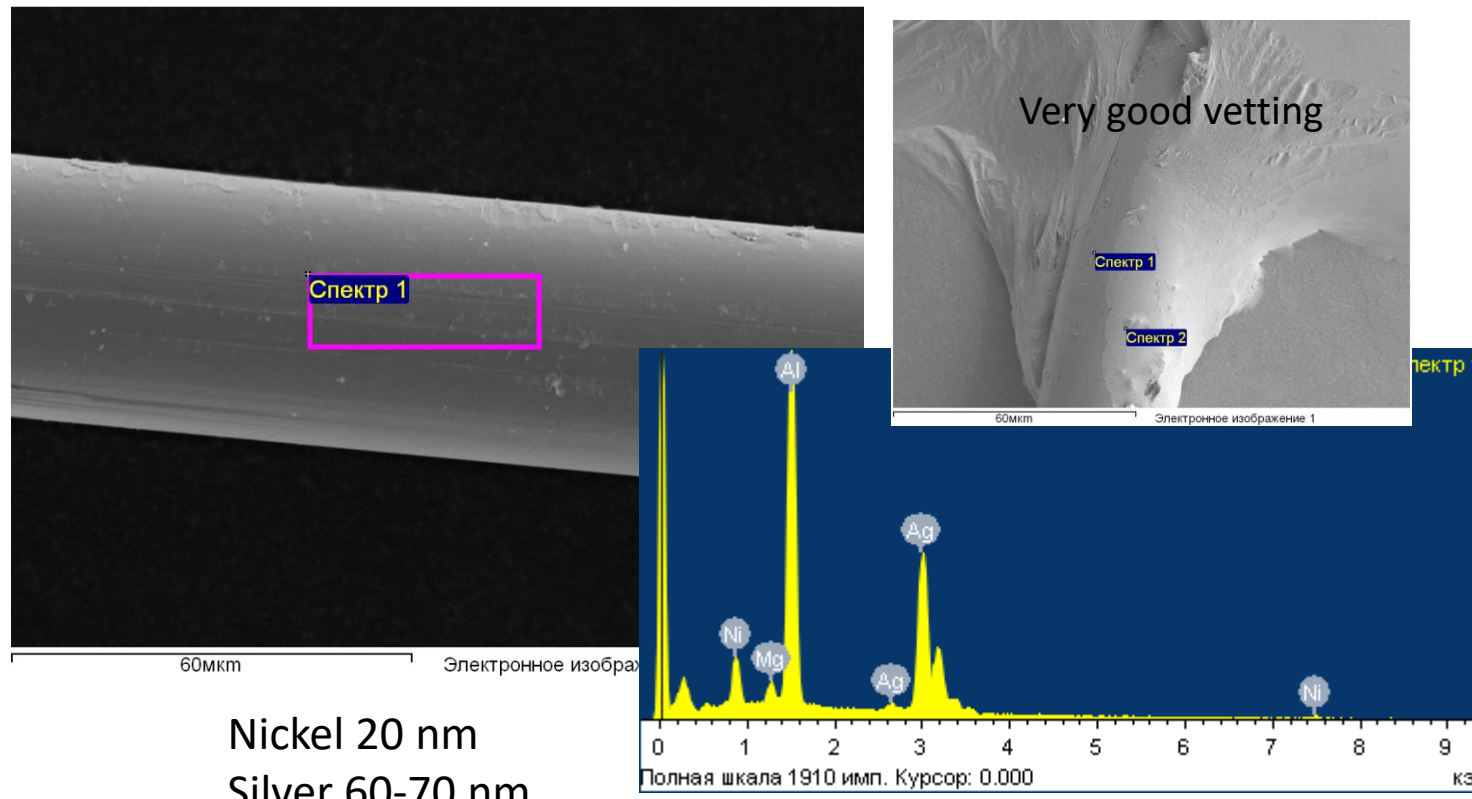
Magnetron coating of wire

Technology for magnetron coating of thin wires (up to 40 μm) has been developed at BINP.

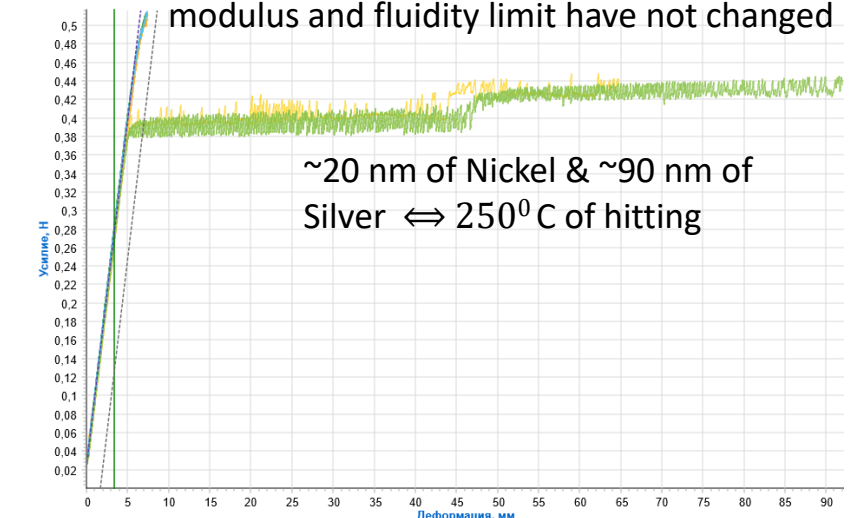


Magnetron coating of wire

Technology for magnetron coating of thin wires (up to 40 μm) has been developed at BINP.



~20 nm of Nickel & ~60 nm of Silver , Young's modulus and fluidity limit have not changed

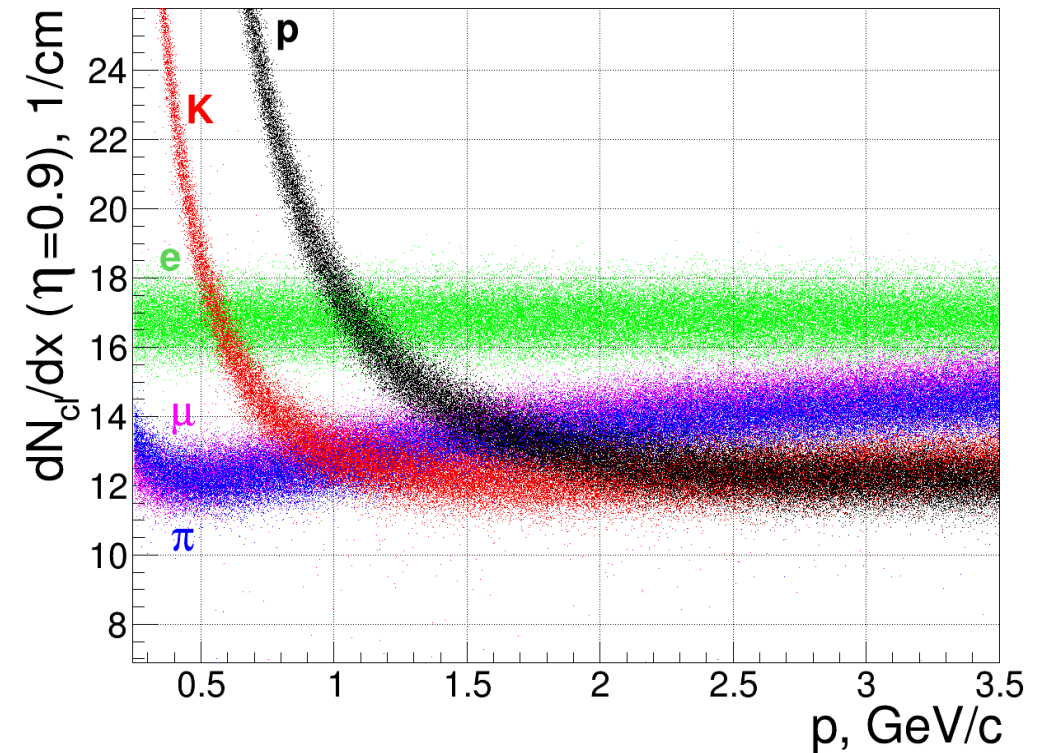
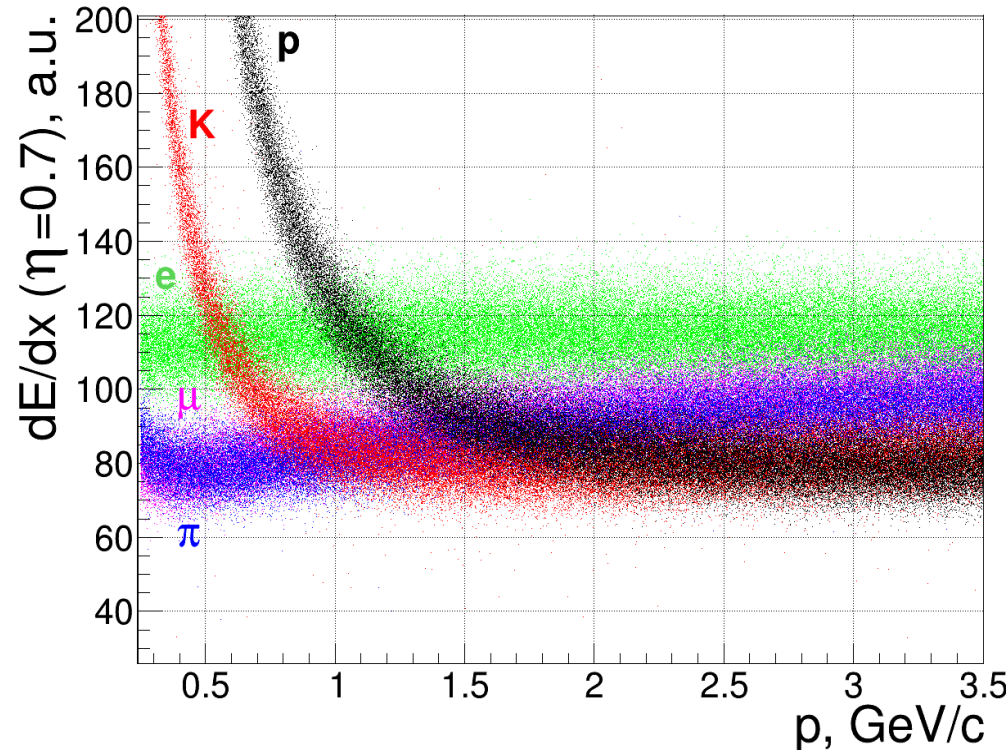


~20 nm of Nickel & ~90 nm of Silver $\Leftrightarrow 250^{\circ}\text{C}$ of hitting

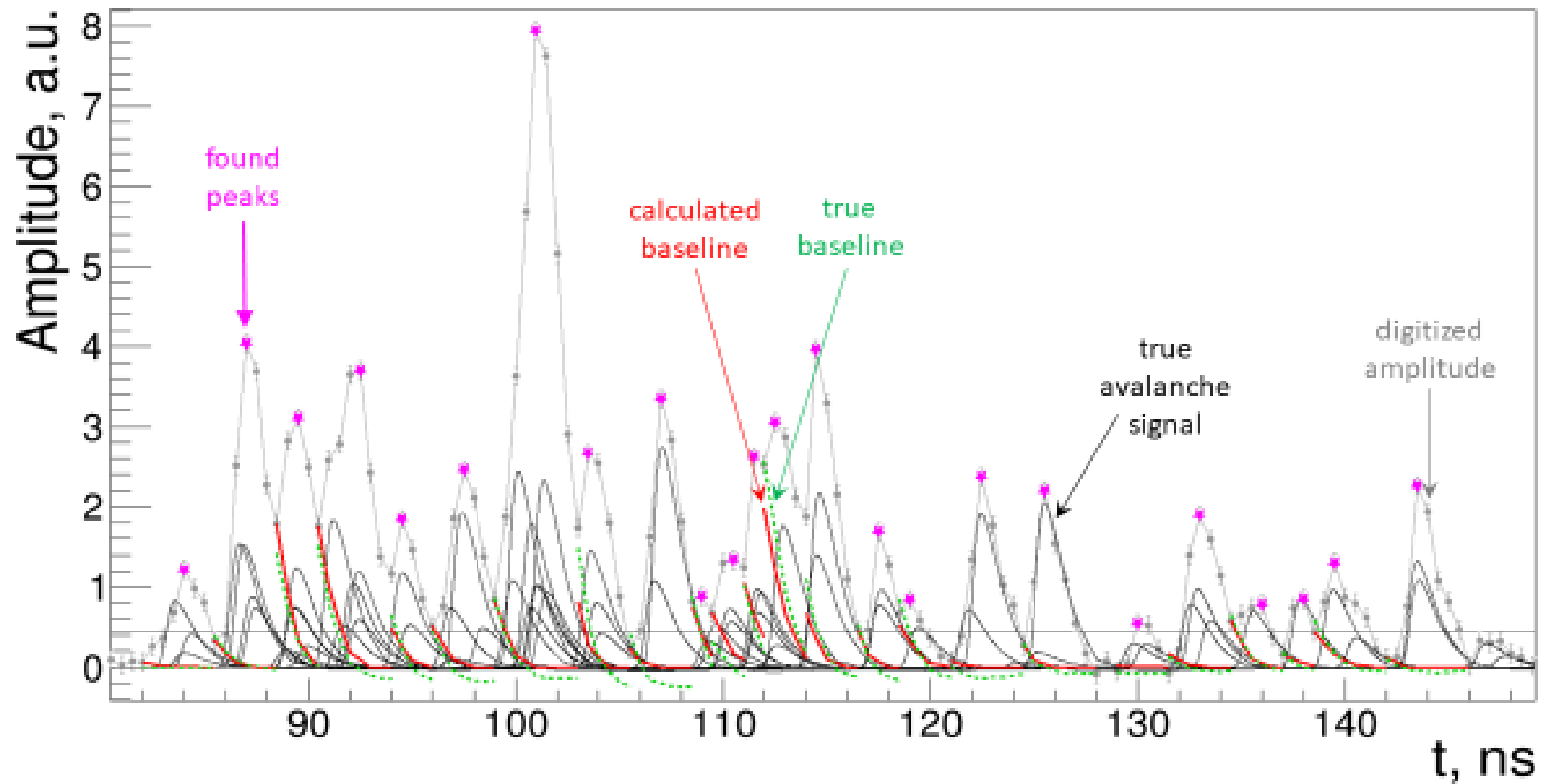
Mechanical properties tests of coated 40-micron wires

Cluster counting

Counting number of ionization clusters (rather than deposited energy) can improve dE/dx resolution up to x2!



Cluster counting – simulations



Cluster counting - test beam at CERN

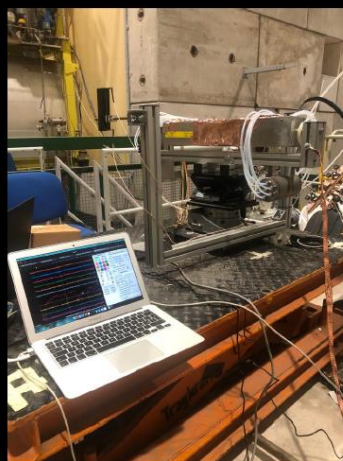
Purpose

- Demonstrate the ability to count clusters at a fixed $\beta\gamma$ (e.g. muons at a fixed momentum – 165 GeV/c) by changing:
 - the cell size (1 – 3 cm)
 - the track angle (0° to 60°)
 - the gas mixture (90/10: 12 cl/cm, 80/20: 20 cl/cm, for m.i.p.)
- Establish the limiting parameters for an efficient cluster counting:
 - cluster density as a function of impact parameter
 - space charge (by changing gas gain, sense wire diameter, track angle)
 - gas gain stability
- Train different cluster counting algorithms

S	Claudio CAPUTO	UC Louvain
R	Federica CUNA	INFN Lecce
E	Nicola DE FILIPPIS	INFN Bari
T	Francesco GRANCAGNOLO	INFN Lecce
F	Matteo GRECO	INFN Lecce
I	Sergey GRIBANOV	BINP Novosibirsk
M	Kurtis JOHNSON	U of Florida
H	Sasha POPOV	BINP Novosibirsk
S	Angela TALIERCIO	UC Louvain
	Shuiting XIN	IHEP Beijing

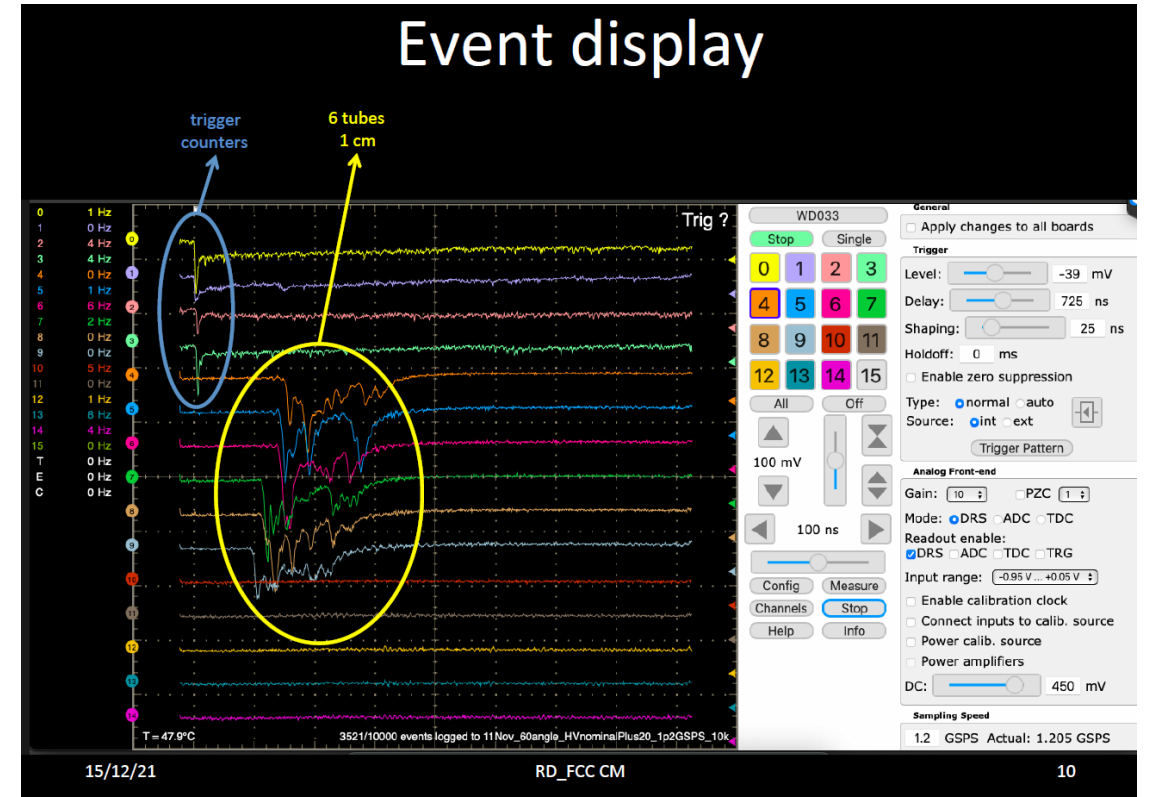
15/12/21

RD_FCC CM



2

Event display



PID

Requirements for PID system

π/K separation $> 4\sigma$ up to 2.5-3.5 GeV/c

TOF (BES-3): 3σ at 0.9 GeV/c, DIRC (BaBar):
 4σ at 2.5 GeV/c

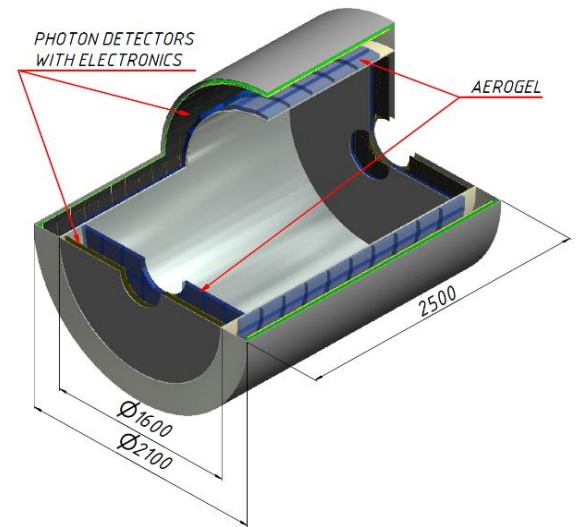
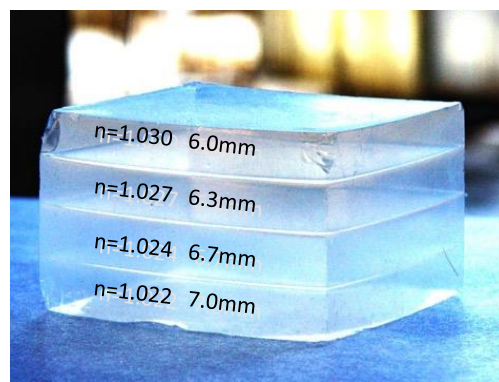
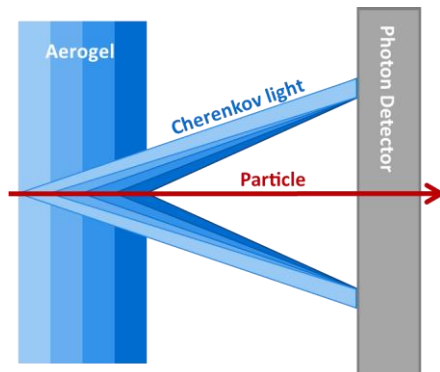
ASHIPH (KEDR): 4σ at 1.5 GeV/c

μ/π suppression $< 1/40$ for 0.5-1.2
GeV/c

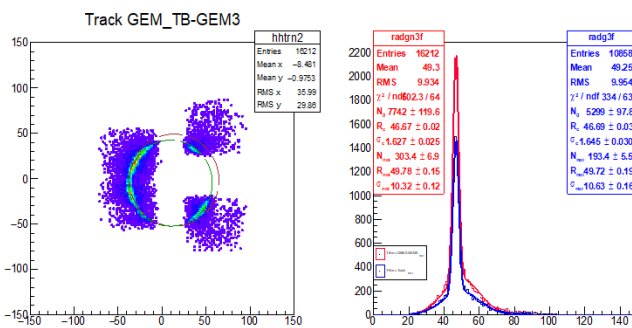
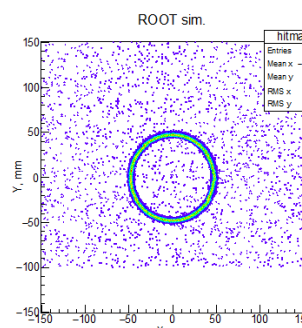
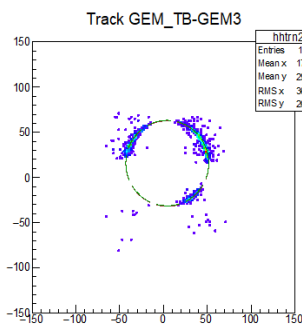
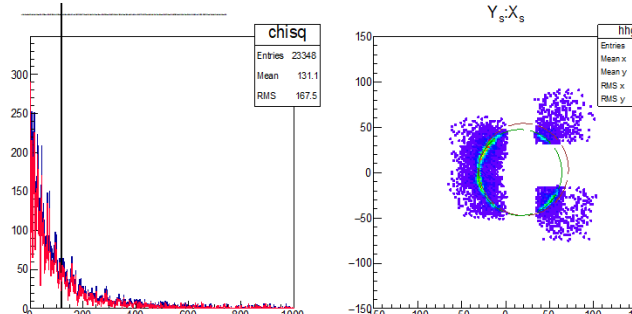
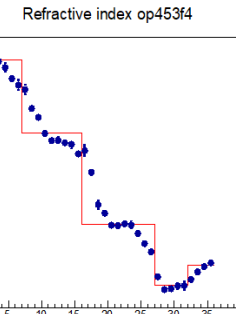
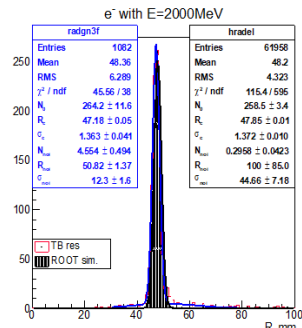
good μ/π separation at low momentum

Several options are being considered:

FARICH, ASHIPH, TOF, FDIRC



FARICH beam tests (2021)



Pixel ϕ 1 mm
 $\sigma_R = 1.36 \pm 0.04 \text{ mm}$

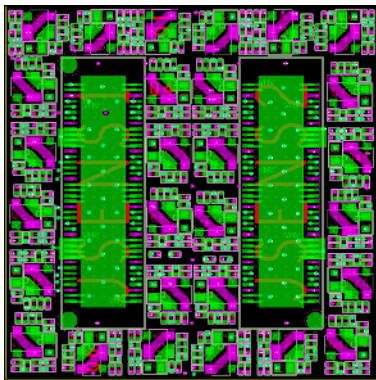
$$\sigma_R^{calc}(\blacksquare 3 \text{ mm}) = \sqrt{1.36^2 + \left(\frac{3}{\sqrt{12}}\right)^2} = 1.613 \text{ mm}$$

Beam test results in May-Dec of 2021 show us that we are very close to target resolution
 $\sigma_R(\blacksquare 3 \text{ mm}) = 1.4 \text{ mm}$ (from G4 simulation)

Pixel ■ 3 mm
 $\sigma_R = 1.63 \pm 0.03 \text{ mm}$

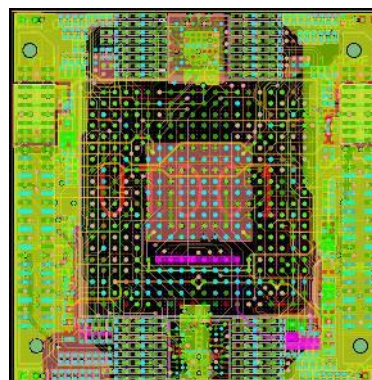
A.Yu.Barnyakov et al., NIMA 1039 (2022) 167044

FARICH: FEE based on FPGA-TDC



Amplifier board

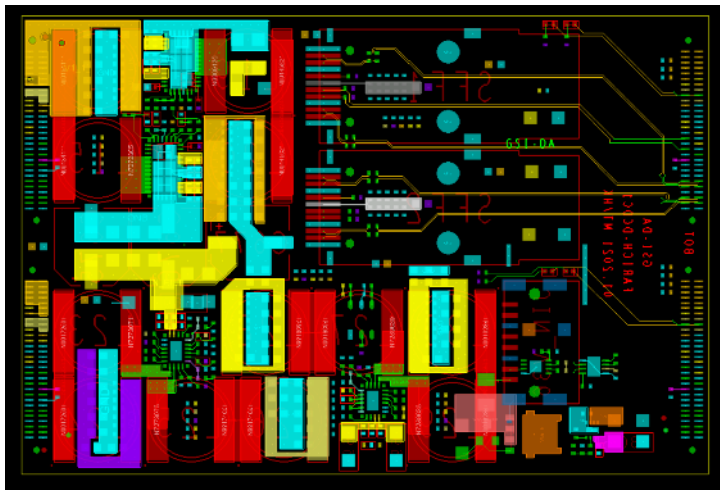
- 27×27 mm² size
- 14-layer PCB
- 30x gain, 64 channels
- couples to KETEK 8×8 SiPM array



TDC board

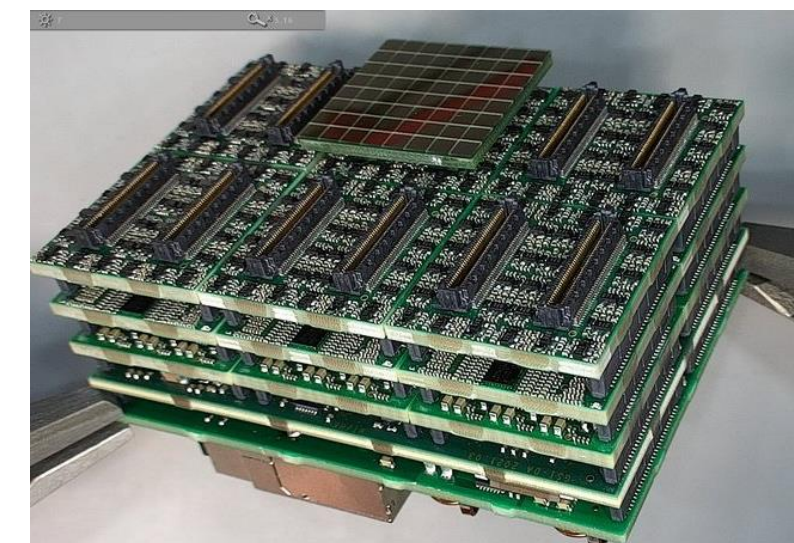
- 64 channels
- 2 TDC + 4 threshold FPGAs
- 10ps precision

- Each module readouts 6 arrays equipped with optical transceiver.
- Thickness of 5-layer design is less than 5 cm.



DC-DC convertor board

- goes behind the backplane
- 51×84 mm² size
- provides power to SiPMs, amplifiers, FPGA
- uses air inductive coils to operate in the detector magnetic field
- power, trigger & clock connectors



Calorimeter

Baseline:

BELLE/BELLE-2-like electromagnetic crystal calorimeter

Scintillator:

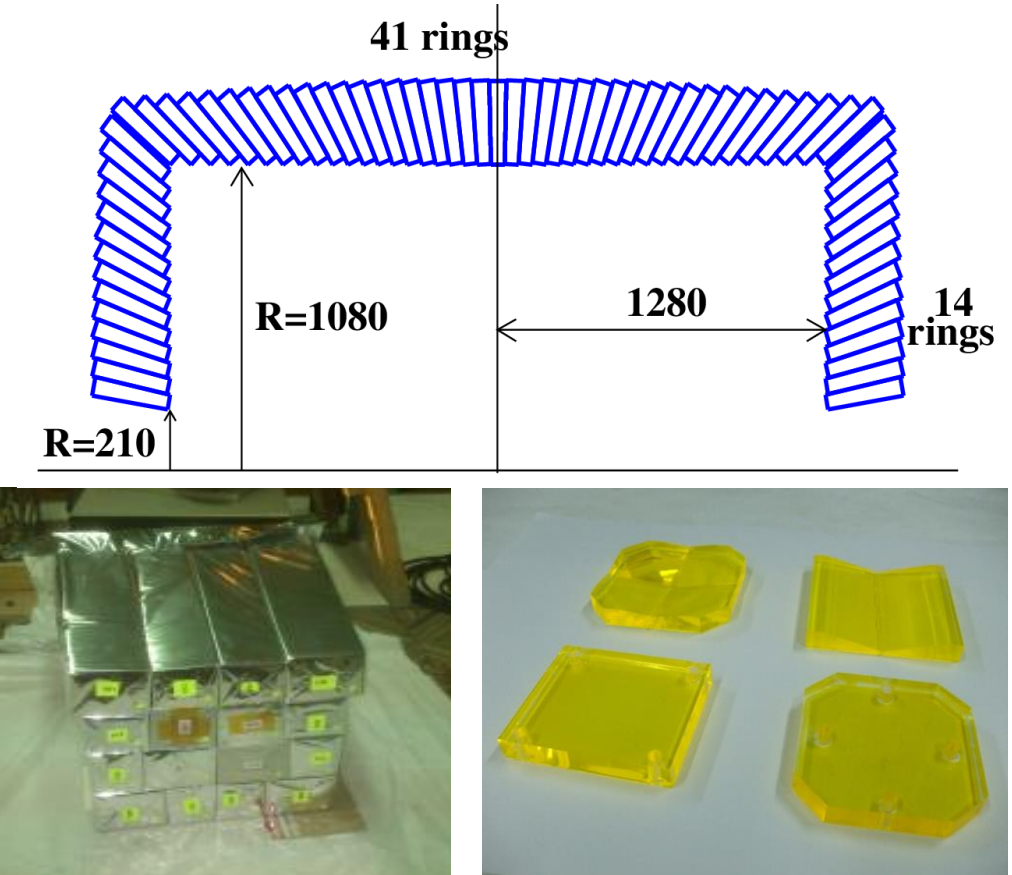
CsI(Tl) has large light yield, “cheap”, very popular – but slow
LSO, LYSO, etc. – have large LY, very fast – but very
expensive (x10)

**pure CsI – good compromise: reasonable LY,
30 ns component, reasonable price**

7424 crystals pCsI + WLS + 4 APD

$$\frac{\sigma_E}{E} \approx \frac{1.9\%}{\sqrt[4]{E(GeV)}} \oplus \frac{0.33\%}{\sqrt{E}} \oplus \frac{0.11\%}{E}$$

There are extensive studies with prototype at BINP.
SiPM readout is being tested as well (as an option to
improve time resolution)



Muon system

- detect muons
 - mult.scat. of $O(1\text{cm})$
- μ/π separation
- K_L detection

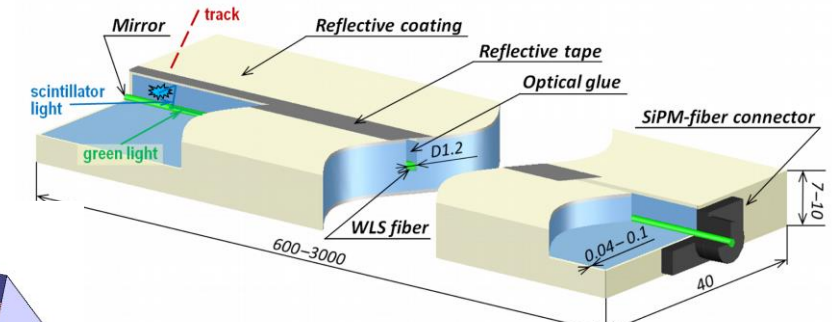
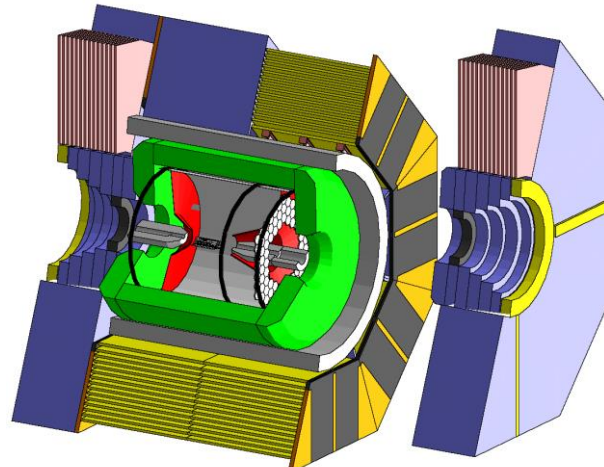
Baseline option:

scintillator strips + WLS fiber + SiPM

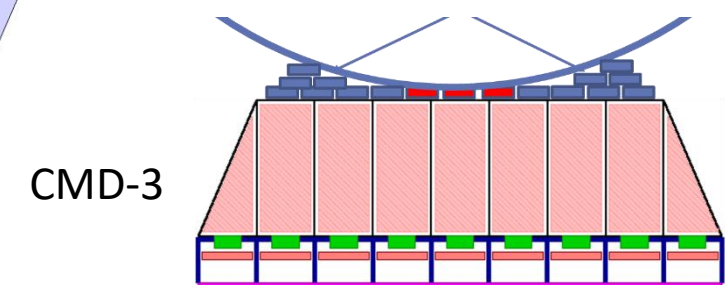
(BELLE-2, CMD-3)

8-9 layers inside iron yoke

$\sim 1500 \text{ m}^2$



BELLE-2



CMD-3

Simulation software

➤ SCT detector software framework

AURORA is released. It includes

- Full geometry description
- Unified description of sensitive detectors
- Realistic magnetic field
- Digitization and reconstruction for some subsystems
- Full parametric simulation
- Basic data analysis tools
- Stack of external software

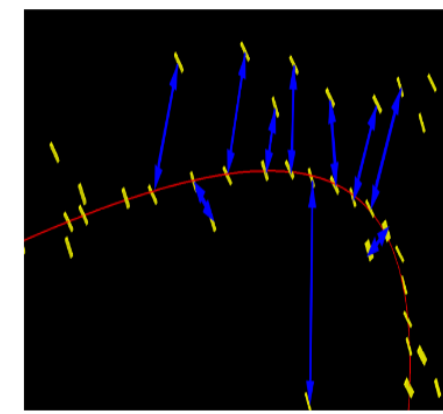
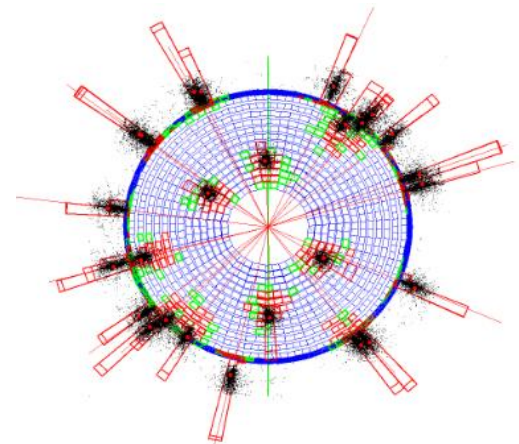
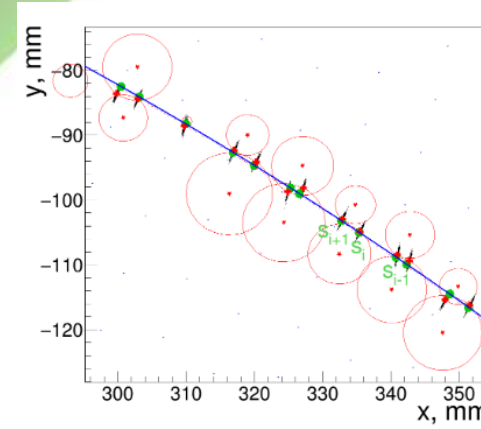
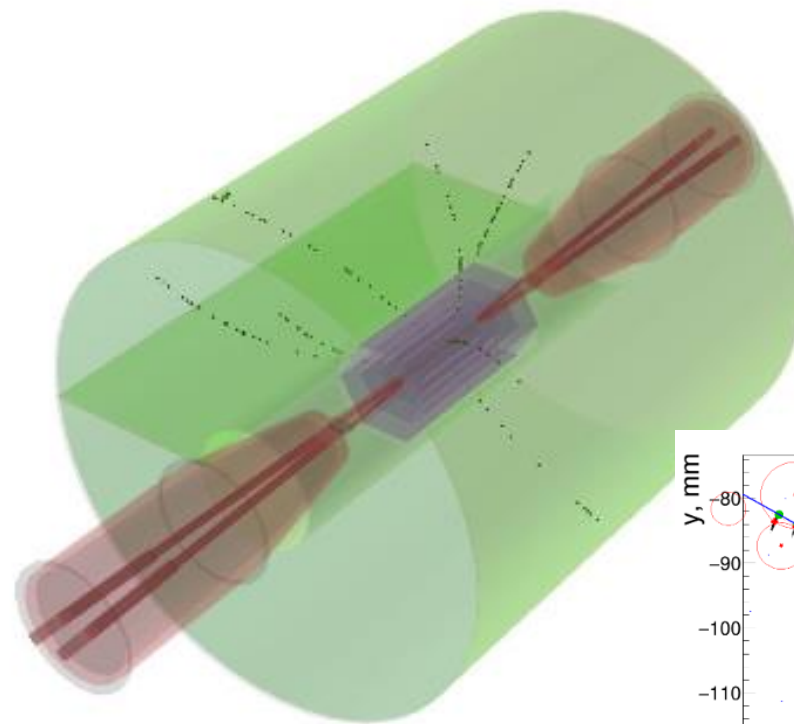
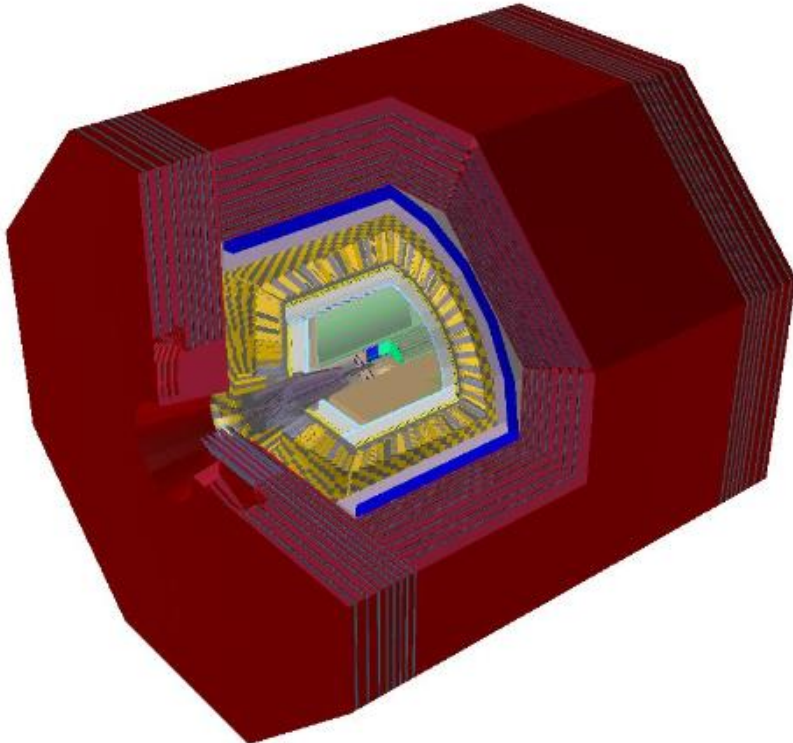
➤ Publications

- Presented at AFAD-2021
- Presented to vCHEP21

Aurora internals:

- Based on Gaudi (de-facto HEP standard)
 - ▶ allows to develop software components in a convenient way (Algorithms, Tools, Services)
 - ▶ mixing C++ and Python code
- Conventional and recently emerged HEP software tools:
 - ▶ ROOT, Geant4...
 - ▶ Key4HEP (DD4hep, PODIO...)
- Other experiments software
 - ▶ Belle II, ILC, FCCSW...
- Build & configuration system inspired by ATLAS Athena
- `lcgcmake` system to build external packages
- Nightly builds
- Standard computing environment is Scientific Linux 7 x86_64, GCC8 + Python2&3

Simulations

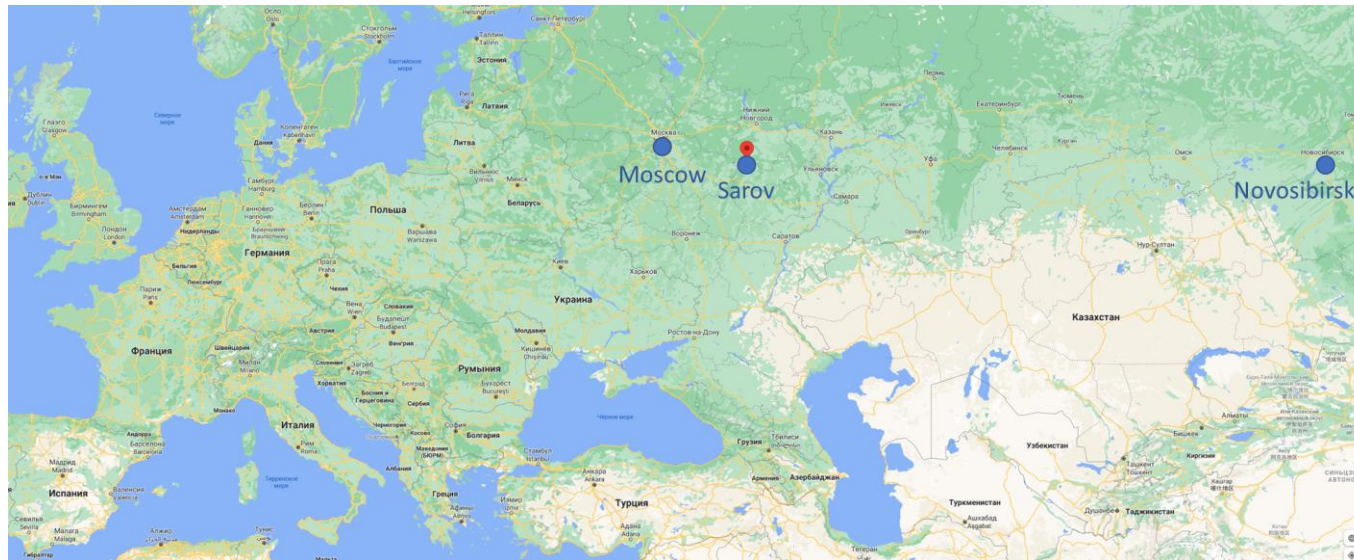


Development supported by RSF grant 19-72-20114

Project

Potential location: Sarov

- National Center of Physics and Mathematics is a new scientific center, located near Sarov
- It includes a branch of Moscow State University (first programs are launched in 2021)
- SCTF is discussed as one of the anchor science infrastructures for NCPM



International workshops

Workshops on future super charm tau factories:

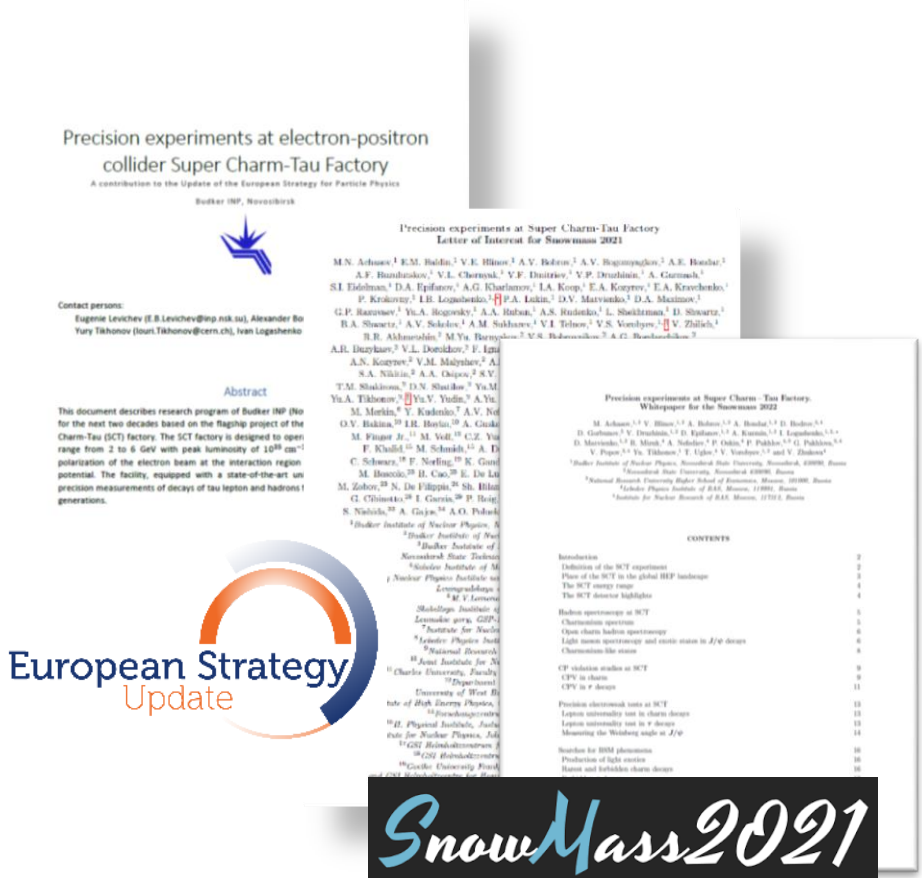
1. December 2017, Novosibirsk ([link](#))
2. March 2018, Beijing ([link](#))
3. May 2018, Novosibirsk ([link](#))
4. December 2018, Orsay ([link](#))
5. November 2019, Moscow ([link](#)) + 1st general WP5 meeting
6. November 2020, Hefei (online, [link](#))
7. November 2021, Novosibirsk (hybrid, [link](#)) as 5th general WP5 meeting

CREMLINplus WP5 meetings: *(CREMLIN+ terminated in April 2022)*

8. 2nd general WP5 meeting, September 2020 (online, [link](#))
9. 3rd general WP5 meeting, February 2021 (online, [link](#))
10. 4th general WP5 meeting, July 2021 (online, [link](#))
11. The SCT Partnership kick-off meeting, November 18th, 2021 ([link](#))



Participation in global strategy forums



European Strategy for Particle Physics Update

- The SCT physics potential is reflected in Physics Briefing book: [arXiv:1910.11775](https://arxiv.org/abs/1910.11775) [hep-ex]

Snowmass2021

- Letter of intent for SCT is signed by 100 colleagues from 38 organizations (including 10 Russian organizations)
 - February 2022: white paper submitted

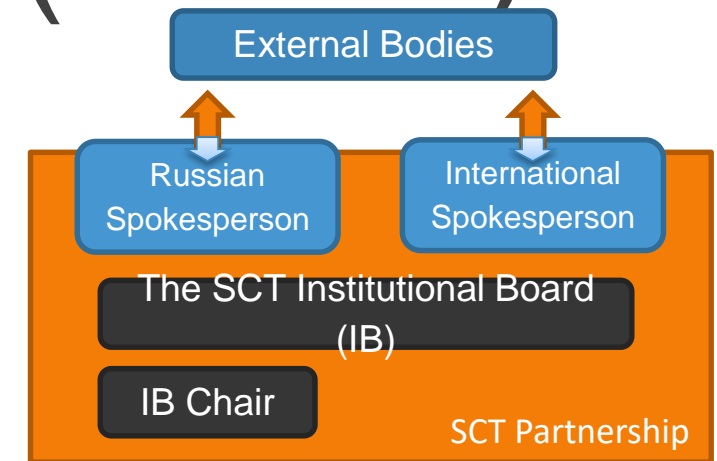
The SCT Partnership (SCTP)



Ivan Logashenko
IB Chair



Pavel Pakhlov
Russian Spokesperson



Proto-collaboration (SCT Partnership) launched in November 2021.

1. Preparation of TDR
 2. Development of the physics program
 3. Shaping future collaboration
- sct.inp.nsk.su/partnership

Ivan Logashenko (BINP)

PHIPSI'2022. Status of Super charm-tau
factory project.

A Annex 1. The Partners

List of all Partners. To be updated each time a new Partner has joined.

Country	Affiliation	LoI signing date
Germany	Justus Liebig University (JLU) Giessen	2021.09.22
Russia	Novosibirsk State Technical University (NSTU)	2021.09.24
Russia	Novosibirsk State University (NSU)	2021.10.11
Russia	P.N. Lebedev Physical Institute of Russian Academy of Science (LPI RAS)	2021.10.11
Russia	Budker Institute of Nuclear Physics (BINP)	2021.10.13
Russia	Lomonosov Moscow State University Skobeltsyn Institute of Nuclear Physics (SINP MSU)	2021.10.29
Mexico	Physics Department, Center for Research and Advanced Studies (Cinvestav)	2021.11.12
International	Joint Institute for Nuclear Research (JINR)	2021.11.15
Russia	Higher School of Economics (HSE) University	2021.11.15
Russia	Institute of Nuclear and Radiation Physics (INRP) RFNC-VNIIEF	2021.11.16

Table 1: Updated on November 18, 2021.

Summary

1. There is rich physics program of experiments at Super c-tau factory
2. There is conceptual design of the Super c-tau factory
3. There are ongoing studies of collider and injector designs, simulations of the experiments at SCTF, developments of the detector subsystems – on the way to TDR
4. The collaboration on the project is growing. The proto-collaboration, SCT Partnership, has been established.
5. There is new possible location for SCTF: the recently established National Center of Physics and Mathematics near Sarov